Journal of Geophysical Research: Earth Surface

RESEARCH ARTICLE
10.1029/2017JF004534

Long-Term Evolution of Sand Transport Through a River Network: Relative Influences of a Dam Versus Natural Changes in Grain Size From Sand Waves

David J. Topping[1], Erich R. Mueller[2], John C. Schmidt[3], Ronald E. Griffiths[1], David J. Dean[1], and Paul E. Grams[1]

[1]Grand Canyon Monitoring and Research Center, U.S. Geological Survey, Flagstaff, AZ, USA, [2]Department of Geography, University of Wyoming, Laramie, WY, USA, [3]Department of Watershed Sciences, Utah State University, Logan, UT, USA

Key Points:
- It should not be generally assumed that sediment transport in a river is in equilibrium with the upstream sediment supply
- Modern physically based analyses of old suspended-sand data can be used to detect the former passage of previously unrecognized sand waves
- Natural changes in grain size from sand-wave migration may influence sand transport more than upstream dam construction

Supporting Information:
- Supporting Information S1-S11

Correspondence to:
D. J. Topping,
dtopping@usgs.gov

Citation:
Topping, D. J., Mueller, E. R., Schmidt, J. C., Griffiths, R. E., Dean, D. J., & Grams, P. E. (2018). Long-term evolution of sand transport through a river network: Relative influences of a dam versus natural changes in grain size from sand waves. *Journal of Geophysical Research: Earth Surface*, *123*, 1879–1909. https://doi.org/10.1029/2017JF004534

Received 27 OCT 2017
Accepted 23 MAY 2018
Accepted article online 19 JUN 2018
Published online 20 AUG 2018

Abstract Temporal and spatial nonuniformity in supplies of water and sand in a river network leads to sand transport that is in local disequilibrium with the upstream sand supply. In such river networks, sand is transported downstream as elongating waves in which coupled changes in grain size and transport occur. Depending on the magnitude of each sand-supplying event and the interval between such events, changes in bed-sand grain size associated with sand-wave passage may more strongly regulate sand transport than do changes in water discharge. When sand transport is controlled more by episodic resupply of sand than by discharge, upstream dam construction may exacerbate or mitigate sand-transport disequilibria, thus leading to complicated and difficult-to-predict patterns of deposition and erosion. We analyzed all historical sediment-transport data and embarked on a 4-year program of continuous sediment-transport measurements to describe disequilibrium sand transport in a river network. Results indicate that sand transport in long river segments can evolve over ≥50-year timescales following rare large sand-supplying events. These natural changes in sand transport in distal downstream river segments can be larger than those caused by an upstream dam. Because there is no way to know *a priori* whether sand transport in a river has changed in response to changes in the upstream sand supply, contemporary continuous measurements of sand transport are required for accurate sand loads and budgeting. Analysis of only historical sediment-transport measurements, as is common in the literature, may lead to incorrect conclusions with respect to current or future sediment-transport conditions.

Plain Language Summary Recognition of the passage of sand waves is critical to river monitoring and management. We use modern suspended-sand analyses conducted on historical data to detect the previously unrecognized passage of large sand waves through a river network. We combine these analyses with a modern continuous sediment-transport measurement program to show that the migration of these sand waves can affect rates of sand transport over timescales exceeding 50 years and in river segments ~260 km in length. The coupled grain-size and transport aspects of the migration of these naturally occurring waves can have a larger impact on sand transport in distal downstream river segments than the construction and operation of a large dam. Without sufficient sand-transport measurements, it is not possible to *a priori* know whether sand transport in a river is controlled by episodic changes in the upstream sand supply. Therefore, in general, continuous contemporary measurements of sand transport are required when initiating sand monitoring in rivers.

1. Introduction

Sources of runoff and sediment are not uniformly distributed in time and/or space in many river networks in semiarid climates (e.g., Andrews, 1991; Howard & Dolan, 1981; Iorns et al., 1964; Schmidt & Wilcock, 2008), volcanic landscapes (e.g., Dinehart, 1998; Gran et al., 2011; Major, 2004), and other mountainous regions (e.g., Benda, 1990; Brummer & Montgomery, 2006; Dietrich & Dunne, 1978). Consequently, main-stem sediment transport in these river networks will be in local disequilibrium with the sediment supply. Moreover, this disequilibrium in sediment transport will be exacerbated in cases where the timing of large sediment-supplying events is episodic, with long intervals of quiescence. When the episodic sediment supply is finer than the antecedent riverbed sediment, the introduced sediment is transported downstream as an elongating sediment wave in which substantial coupled changes in grain size and sediment transport occur (Cui, Parker, Lisle, et al., 2003; Cui, Parker, Pizzuto, et al., 2003; Ferguson et al., 2015; James, 2010; Lisle, 2007;

Topping, Rubin, Nelson, et al., 2000; Wohl & Cenderelli, 2000). The topographic signature of a sediment wave in some cases may be small (Ferguson et al., 2015), with the downstream migration of a sediment wave being evident mainly in its effects on the transported sediment and the grain-size distribution of the bed (Topping, Rubin, Nelson, et al., 2000; Topping, Rubin, & Vierra, 2000). Recognition that sediment transport has responded or is responding to the passage of a sediment wave is critical to river monitoring and management (James, 2006, 2010). It can be particularly difficult to detect the former passage of sediment waves when the legacy of such waves primarily consists of their effects on grain size and sediment transport, and not their effects on river form. In addition, because repeat topographic data may not be available, it is generally important to develop methods to detect the former passage of sediment waves using only sediment-transport and grain-size data.

We use a variety of analyses of historical and modern data to investigate a river network dominated by disequilibrium sediment transport. Specifically, we demonstrate that the passage of large sand waves through a river network can be detected using a suite of physically based analyses of water discharge and sand transport in a case where no topographic data were available. We show that the passage of such hard-to-detect waves has affected sand transport in a ~260-km-long river segment over ≥50-year timescales and that long-term changes in sand transport caused by natural sand-wave migration can exceed those caused by dam construction. Analyses of discharge data were used to detect sand-wave initiation during tributary floods and to detect changes in main-stem flow that could affect sand transport. Analyses of suspended-sand data were used to detect the downstream propagation of the coupled grain-size and transport signature of sand-wave migration.

1.1. Study Area

The study area is the network of the Green and Yampa rivers that merge within Dinosaur National Monument to form the middle Green River (Figure 1). This area encompasses (1) the Green River between Green River, WY, and Jensen, UT; (2) the Yampa River downstream from Maybell, CO; (3) the Little Snake River; and (4) smaller tributaries (Figure 1). The Green River is divided into "upper" and "middle" segments at its confluence with the Yampa River, which in turn is divided into "upper" and "lower" segments at its confluence with the Little Snake River. Most of the streamflow is supplied by snowmelt upstream from the study area, whereas most of the sand is supplied episodically by tributaries within the study area (Andrews, 1978, 1980; Resource Consultants, 1991; U.S. Environmental Protection Agency, 2014). Upstream water development has affected only half of the study area (Andrews, 1986), creating a natural laboratory where changes in sand transport caused by water development can be compared with those caused by natural processes.

The upper Green River has been regulated since 10 December 1962, when Flaming Gorge Dam was closed (Linenburger, 1998). There are no large diversions downstream from this dam in the study area, but there are large dams and diversions upstream, chiefly Fontenelle Dam—constructed between 1962 and 1964 (Linenburger, 1997). Reservoir operations at Flaming Gorge Dam have flattened the annual hydrograph of the upper Green River by reducing the annual snowmelt flood and increasing base flows (Grams & Schmidt, 1999, 2002; Vinson, 2001). Beginning in 2012, these operations were modified and a small spring flood was released for endangered native fish (Bestgen et al., 2011; LaGory et al., 2012; U.S. Bureau of Reclamation, 2006; U.S. Department of the Interior, 2005).

The Yampa and Little Snake rivers are relatively unregulated, and their flow regimes are still dominated by the snowmelt flood (Grams & Schmidt, 2002; Manners et al., 2014). Small dams, transbasin diversions, and other human uses deplete ~13% of the long-term average natural flow (Colorado Water Conservation Board & Colorado's Decision Support Services, 2009a, 2009b; U.S. Bureau of Reclamation, 2016; U.S. Department of Agriculture, 1981; Wyoming Water Planning Program, State Engineer's Office, 1978). The flow regime of the middle Green River thus has characteristics of the highly regulated upper Green River and the quasi-natural Yampa River (Grams & Schmidt, 2002).

Construction of Flaming Gorge Dam cut off the sand supplied to the study area from most of the upper Green River watershed. Thus, the only major sources of sand to the upper Green River after 1962 were from erosion of predam sand from the riverbed and banks in Browns Park or from Red and Vermillion creeks (Figure 1; Andrews, 1986; Grams & Schmidt, 2005; Mueller, Grams, Schmidt, Hazel, Alexander, et al., 2014; Mueller, Grams, Schmidt, Hazel, Kaplinski, et al., 2014). After dam completion, the Yampa River became the primary

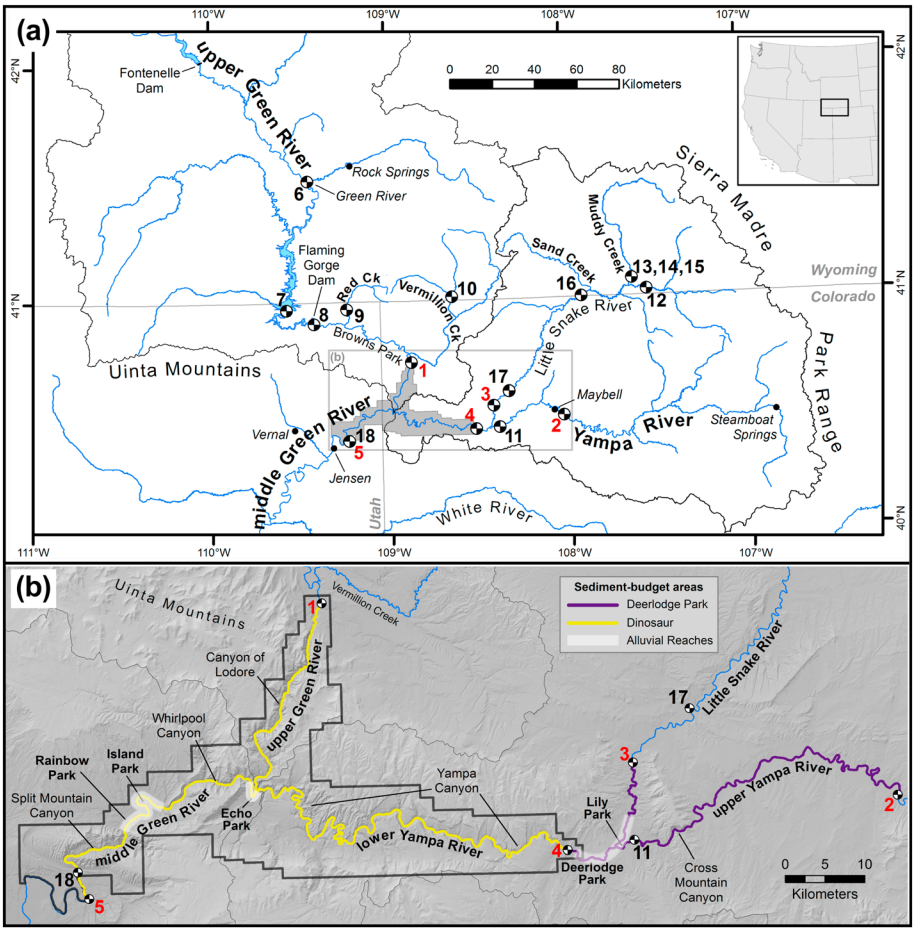

Figure 1. Maps of the study area depicting the river segments, geographic features, and sediment-budget areas referred to herein. Shown are the gaging stations (black and white checkered circles) at which data were collected; numbers are keyed to the abbreviated gaging station names in Table 1 (red numbers indicate primary gaging stations, and black numbers indicate ancillary gaging stations). Gray-shaded region in (a) indicates extent of Dinosaur National Monument; gray box around this area indicates extent of (b), in which the river segments and shorter alluvial reaches in each sediment-budget area are depicted.

source of sand to the middle Green River, with most of this sand supplied by tributaries that drain into the lower Little Snake River (Andrews, 1978, 1980, 1986; Grams & Schmidt, 2005).

1.2. Previous Sediment Transport Research in the Study Area

Previous sediment-transport and budgeting research in the study area relied on analyses of preexisting suspended-sediment data sets (Andrews, 1978, 1980, 1986; Grams & Schmidt, 2005; Resource Consultants, 1991) or sediment rating curves fit to short-term data sets (Elliott & Anders, 2005; Elliott et al., 1984; O'Brien, 1984; Resource Consultants, 1991) to infer contemporary or future sediment conditions. Interpretations of these data were hindered by a lack of overlap between periods of sediment record among gaging stations and from large intra-annual and interannual variability in sediment transport, potentially resulting in highly biased mean-annual sediment loads. For example, Andrews (1986) and Grams and Schmidt (2005) arrived at differing conclusions as to the signs of postdam sediment budgets for the Green River.

1.3. Locations and Periods of Data Collection

We segregated sediment data into pre-2012 "historical" and 2012–2016 "modern" periods. To avoid the limitations of previous studies, we continuously measured sediment transport during 2012–2016 at five "primary" gaging stations where the U.S. Geological Survey (USGS) had collected data between 1947 and 2011

Journal of Geophysical Research: Earth Surface

10.1029/2017JF004534

Table 1

Periods of Discharge, Suspended-Sediment, and Bedload Record at the USGS Gaging Stations in This Study

Official USGS gaging station name and number	Station number in Figure 1 and abbreviated station name used in this paper	Daily mean *Q* and annual peak *Q*	Historical episodic suspended-sediment measurements with grain-size analysis of the sand fraction	Historical daily sediment loads published by the USGS on the basis of quasi-daily suspended-sediment measurements	Historical episodic grain-size-analyzed bedload measurements paired with suspended-sediment measurements	Modern period of continuous 15-min suspended-sediment measurements
Primary gaging stations						
Green River above Gates of Lodore, CO, 404417108524900	1. Green-Lodore	July 2012, October 2012–ongoing	July 1995–June 1997[c], April 2000–June 2002	na	July 1995–June 1997[c] May 1999–June 2002	July 2012, October 2012–ongoing
Yampa River near Maybell, CO, 09251000	2. Yampa-Maybell	May 1916– ongoing	April 1951–May 1982	December 1950–May 1958, October 1975–November 1976, October 1977–September 1983	na	March 2013–ongoing
Little Snake River near Lily, CO, 09260000	3. LS-Lily	October 1921–ongoing	April 1958–September 1958, June 1978–July 2011	May 1958–September 1958	March 2001–June 2002	March 2013–ongoing
Yampa River at Deerlodge Park, CO, 09260050	4. Yampa-Deerlodge	October 1982–ongoing	April 1982–July 2011	na	April 1982– June 2001	October 2012–ongoing
Green River near Jensen, UT, 09261000	5. Green-Jensen	October 1946–ongoing	April 1951–May 2007	May 1948–September 1979	May 1996–July 2002	March 2013–March 2016
Ancillary gaging stations						
Green River near Green River, WY, 09217000	6. Green-Green River	October 1951–ongoing	May 1951–June 1991	May 1951–September 1992	na	na
Green River near Linwood, UT, 09225500	7. Green-Linwood	October 1929–March 1963	na	na	na	na
Green River near Greendale, UT, 09234500	8. Green-Greendale	October 1950–ongoing	May 1958–September 1958	October 1956–September 1958[e]	na	na
Red Creek near Dutch John, UT, 09234700	9. Red Creek	February 1972–September 1976	February 1971–August 1976	February 1971–September 1976	na	na
Vermillion Creek near Hiawatha, CO, 09235300	10. Vermillion Creek	October 1975–September 1981	May 1976–May 1981	na	na	na
Yampa River above Little Snake River near Maybell, CO, 09251100	11. Yampa-above LS	May 1996–September 2003	May 1998–July 2011	na	May 1998–June 2002	na
Little Snake River near Dixon, WY, 09257000	12. LS-Dixon	October 1910–September 1923,October 1938–September 1997[b], September 2014–ongoing	March 1972–May 1988[d]	na	na	na
Muddy Creek above Baggs, WY, 09258900	13. Muddy-above Baggs	October 1957–September 1971 (annual peak *Q* only)	na	na	na	na
Muddy Creek below Young Draw, near Baggs, WY, 09258980	14. Muddy-Young	April 2004-ongoing	na	na	na	na
Muddy Creek near Baggs, WY, 09259000	15. Muddy-Baggs	October 1987–September 1991	March 1988	March 1988–September 1990	na	na
Little Snake River near Baggs, WY, 09259700	16. LS-Baggs	October 1961–September 1968	na	na	na	na
Little Snake River above Lily, CO, 09259950[a]	17. LS-above Lily	na	October 1959–September 1964	October 1959–September 1964	na	na
Green River above Jensen, UT	18. Green-above Jensen	na	na	na	na	April 2016–ongoing

[a]Sediment loads published for this station used *Q* at the LS-Lily station located 14 km downstream. [b]Daily mean *Q* not calculated during ice-affected months from October 1971 through April 1997. [c]Utah State University and National Park Service measurements (Martin et al., 1998); pre-1997 measurements were not processed for silt and clay concentration. [d]One hundred one measurements were made between October 1971 and October 1982 and during May–June 1988, but only 8 were analyzed for grain size; suspended-sediment concentration among the 101 samples was typically low with a median value of 40 mg/L, a mean value of 150 mg/L, and a maximum value of 1,200 mg/L. [e]Sediment loads during water year 1957 (October 1956 through September 1957) were published by the USGS as monthly loads.

(Figure 1 and Table 1). We analyzed all discharge (Q), sediment-transport, and bed-sediment data at these stations, and we also analyzed historical Q and sediment-transport data at 12 ancillary gaging stations (Figure 1 and Table 1).

2. Field Methods

Accurate sediment-load calculation requires near-continuous velocity-weighted measurements of suspended-sediment concentration (C) in a river cross section (Gray & Gartner, 2009; Gray & Simoes, 2008; Porterfield, 1972; Topping et al., 2000; Topping & Wright, 2016). These measurements are termed velocity-weighted because they are made using isokinetic depth-integrating suspended-sediment samplers that collect the water–suspended-sediment mixture at the local flow velocity (Edwards & Glysson, 1999; Federal Interagency Sedimentation Project, 1952). When velocity-weighted C is measured by the Equal-Width-Increment (EWI) method, multiplication of C by Q yields the suspended-sediment flux (Edwards & Glysson, 1999). Integration of this flux over time then yields the sediment load (Porterfield, 1972). The USGS measured Q at each gaging station using standard methods (Blanchard, 2007; Rantz et al., 1982a, 1982b; Turnipseed & Sauer, 2010), with 15-min Q available since water year 2008. Historically, the USGS published sediment loads using quasi-daily EWI measurements (Osterkamp & Parker, 1991), with occasional grain-size-analyzed measurements made to allow load estimation by size class. In the modern period, we computed sediment loads using 15-min acoustical suspended-sediment measurements calibrated and verified with EWI and calibrated-pump measurements (methods developed from theory by Topping & Wright, 2016; Topping et al., 2016). Historically, bedload was measured using Helley-Smith samplers (Elliott & Anders, 2005; Elliott et al., 1984; Martin et al., 1998); we calculated bedload on the basis of bedform migration (after Simons et al., 1965).

Bed-sediment measurements were made more systematically during 2012–2016 than historically, and none were made anywhere before 1982. We made bed-sediment measurements paired with EWI measurements at the sand-bedded Green-Lodore, LS-Lily, and Yampa-Deerlodge stations, but not at the gravel-bedded Yampa-Maybell and Green-Jensen stations.

Details of measurement methods, references, and site-specific issues are provided in Text S1 and S3 in the supporting information. All data collected since 2012, with user-interactive plots and sediment budgets, are available at https://www.gcmrc.gov/discharge_qw_sediment/ or https://cida.usgs.gov/gcmrc/discharge_qw_sediment/ (Sibley et al., 2015).

3. Analytical Methods

We focused our analysis on sand, rather than silt and clay, because of the much greater interaction of suspended sand with the riverbed (e.g., Andrews, 1981; Guy, 1970). The upstream sand supply interacts with the flow to cause changes in suspended-sand concentration (C_{SAND}) coupled with changes in the grain-size distribution of the bed and suspended sand (e.g., Rubin & Topping, 2001, 2008; Rubin et al., 1998; Topping, Rubin, Nelson, et al., 2000; Topping, Rubin, & Vierra, 2000; Topping et al., 2007, 2010). Because silt and clay are typically transported as wash load, changes in the upstream silt and clay supply generally cause changes in suspended-silt-and-clay concentration without causing major changes in the bed sediment. Silt-and-clay analyses parallel to some of our sand analyses are provided in Text S11.

We analyzed Q data sets to evaluate temporal trends and patterns in Q and tributary sand-supplying events. We then analyzed suspended-sand data sets using α-β analyses—derived from theory and tested using flume and river data by Rubin and Topping (2001, 2008). β analyses were used to track changes in the bed-sand grain-size distribution. α analyses were used to identify stations and periods where the temporal changes in bed-sand grain size associated with possible sand-wave migration played an important role in regulating C_{SAND}. We then linked changes in β and α to changes in the relations between Q and C_{SAND}. Finally, we computed sand loads and budgets for different parts of the study area. Significant temporal trends (at the $p < 0.05$ level of significance) were detected using F tests on least-squares linear regressions (e.g., Davis, 1986). Significant ($p < 0.05$) differences between data from different periods were detected using Wilcoxon-Mann-Whitney (WMW) tests (Mann & Whitney, 1947), chosen over t tests because WMW tests do not require that data be normally distributed.

3.1. Changes in Water Discharge

We evaluated whether long-term trends or patterns relevant for sand transport existed in annual mean and peak Q at the Green-Green River, Green-Greendale, Yampa-Maybell, LS-Lily, and Green-Jensen stations. Time series from the Green-Linwood and Green-Greendale stations were merged to extend the period of the Green-Greendale station (Text S4). Inspection of time series smoothed over 3 years was used to identify changes in interannual Q variability.

3.2. Identification and Timing of Large Sand-Supplying Events to the Little Snake River

Previous studies showed that tributaries to the lower Little Snake River are the source of most of the sediment transported by the Yampa River (Andrews, 1978, 1980; Resource Consultants, 1991). We sought to identify the timing of large floods in these tributaries that delivered large amounts of sand to the downstream river network. Because these tributaries contribute little to annual Q at the LS-Lily station, the analyses of section 3.1 will not likely detect these floods. The largest of these tributaries are Muddy Creek, which is perennial, and Sand Creek, which is ephemeral (Figure 1). Sand Creek has never been gaged, whereas Muddy Creek was gaged by the USGS from 1958 to 1971, 1988 to 1991, and 2004 to present (Table 1).

Owing to its location closer to population and its perennial nature, Muddy Creek has received the most study of any lower Little Snake River tributary (Dolan & Wesche, 1987; Parker et al., 1985; U.S. Environmental Protection Agency, 2014). The largest documented flood on Muddy Creek (peak Q = 75 m^3/s) occurred on 27 March 1962 (Text S5; U.S. Geological Survey, 2017a), with other notable, but much smaller, floods occurring in 1966 and 1971 (U.S. Geological Survey, 2017a, 2017b, 2017c). Parker et al. (1985) documented channel incision resulting from large floods sometime after 1905. In the 1990s, U.S. Environmental Protection Agency (2014) conducted a wetlands-restoration project to mitigate erosion from head cutting during large floods in the 1960s (U.S. Environmental Protection Agency, 2014). The relatively large amount of information available for Muddy Creek, however, does not indicate that it is the largest supplier of sand to the lower Little Snake River. Thus, development of another method was required to comprehensively and objectively identify the sources and timing of large floods in Little Snake River tributaries.

We met this objective by examining streamflow records from bracketing gaging stations on the Little Snake River and by examining the limited streamflow records from Muddy Creek (Figure 1). The gaging stations on the Little Snake River used in these analyses were the LS-Dixon station (~15 km upstream from Muddy Creek) and the LS-Baggs station (~7.4 km downstream from Sand Creek). There are no other major tributaries between these stations; thus, major increases in Q between these stations are caused by floods in Sand and/or Muddy creeks. Months in which large tributary floods occurred were identified as those with the largest average increase in the monthly peak daily mean Q between these stations. Because only 7 years of overlap exist among the LS-Dixon and LS-Baggs stations, we conducted an identical analysis between the LS-Dixon and LS-Lily stations (63 years of June–September overlap and 37 years of November–March overlap). We also conducted an identical analysis between the LS-Baggs and LS-Lily stations (7 years of overlap) to determine the sand-supplying importance of tributaries entering the Little Snake River downstream from the LS-Baggs station.

3.3. β Analyses

The sparseness of historical bed-sediment measurements limits their use in detecting trends in bed-sand grain size. Thus, we used the physically based β analyses of Rubin and Topping (2001, 2008) to estimate bed-sand grain size from suspended-sand measurements. Rubin and Topping (2001, 2008) derived β using suspended-sediment theory and then tested β using bed-sand grain-size distributions measured in flume and river experiments. As defined by Rubin and Topping (2001, 2008),

$$\beta = \frac{D_B}{D_{B\text{-}REF}} = \left(\frac{C_{SAND}}{C_{SAND\text{-}REF}}\right)^{-0.1}\left(\frac{D_S}{D_{S\text{-}REF}}\right) \quad (1)$$

is a nondimensional relative measure of the coarseness of the suspendable bed sand, where D_B is the spatially averaged median grain size (D_{50}) of the bed sand "sampled" by the river via physical suspension processes in the reach upstream from a single EWI measurement, $D_{B\text{-}REF}$ is the reference D_{50} of the bed sand, C_{SAND} is the suspended-sand concentration in a single EWI measurement, $C_{SAND\text{-}REF}$ is the reference suspended-sand concentration, D_S is the D_{50} of the suspended sand in a single EWI measurement, and

$D_{S\text{-}REF}$ is the reference D_{50} of the suspended sand. These reference values are the mean values over the period analyzed. We then evaluated whether detected trends in β reflected measured changes in the bed sand. β analyses were conducted at the five primary gaging stations and at the Green-Green River station. This ancillary station provided predam context for the upper Green River because of insufficient data at the Green-Greendale station and no predam data at the Green-Lodore station.

Depending on Rouse number, β will track D_B, the fine tail of the bed-sand grain-size distribution, or both. For a given flow condition (i.e., constant depth, shear velocity (u_*), and skin-friction boundary shear stress), D_S results from the combined influence of D_B and the fractional amount of each size class comprising the bed-sand grain-size distribution (after Garcia & Parker, 1991; McLean, 1992; Parker, 1978; Rouse, 1937; Schmeeckle, 2014; Smith & McLean, 1977; Topping et al., 2007; van Rijn, 1984a). Thus, for a given flow condition and constant D_B, D_S will be finer and β will be smaller when the bed-sand grain-size distribution is broader or more left-skewed because relatively more sand is present in the finer size classes (i.e., the most suspendable size classes with the lowest Rouse numbers). Therefore, although, as in the Rubin and Topping (2001, 2008) definition of β in equation (1), β tracks D_B when the Rouse number of D_B is relatively low (Rubin & Topping, 2001, 2008; Topping et al., 2010), β may not track D_B when the Rouse number of D_B is $>>1$. Under such coarse-bed conditions, as in the rivers in our study, β is more sensitive to changes in the fine tail of the bed-sand grain-size distribution than it is to changes in D_B (Text S6). β provides a good estimate of bed-sand grain size because the bed-sand grain-size distribution provides a much stronger and nonlinear control on C_{SAND} than does the areal coverage of sand on the bed (Topping et al., 2007). Hence, a factor of 2 change in bed-sand area corresponds to only a ~7% change in β (Topping et al., 2010).

3.4. α Analyses

The two dominant regulators of C_{SAND} are Q and the bed-sand grain-size distribution (after Dean et al., 2016; Grams et al., 2013; Rubin & Topping, 2001; Topping et al., 2000, 2007, 2010). Under constant bed-sand grain size, an increase in Q will cause an increase in u_* and therefore also an increase in C_{SAND}; similarly, under constant u_*, bed-sand fining through a decrease in D_B and/or an increase in the fine tail will cause an increase in C_{SAND}. Thus, we treat bed-sand grain size as an independent variable for the purposes of this paper. Following Rubin and Topping (2001) and using the language of Einstein and Chien (1953), this approach is justified because changes in bed-sand grain size have a "strong and immediate" effect on C_{SAND}, whereas changes in the sand flux (from changes in the upstream sand supply) have only a "weak and slow" influence on the bed-sand grain size.

α analyses (Rubin & Topping, 2001) were used to determine the stations and periods where C_{SAND} was regulated primarily by changes in Q or by changes in the bed-sand grain-size distribution. We used the same data analyzed for β, with the addition of the EWI measurements from the Green-Greendale station to provide predam context for the Green-Lodore station. α analyses were conducted on the entire period of record and on shorter discrete periods determined by temporal changes in β and large gaps between EWI measurements. As derived by Rubin and Topping (2001) from suspended-sediment theory,

$$\alpha = \left(\frac{K}{J+1}\right)\frac{-L\left(\frac{\log_{10}\Delta C_{SAND}}{\log_{10}\Delta D_S}\right)+J}{M\left(\frac{\log_{10}\Delta C_{SAND}}{\log_{10}\Delta D_S}\right)-K} \tag{2}$$

where Δ signifies the ratio of either C_{SAND} or D_S at two different times, $J = 3.5$, $K = -2.5$, $L = 0.35$, and $M = 0.75$. The values of J, K, L, and M were determined from the output of a suspended-sand model and by integral constraints among these variables (Rubin & Topping, 2001; Topping et al., 2010). Equation (2) applies to all cases of varying D_S; equations 4, 6, and 7 in Rubin and Topping (2001) must be used to solve for α in the special case of constant D_S.

α is a quantitative measure of the relative importance of changes in u_* and changes in D_B in regulating C_{SAND} (Rubin & Topping, 2001) and is therefore also a measure of the degree to which sand transport is in disequilibrium with the upstream sand supply. The sign of α is unimportant. α is defined such that changes in u_* and D_B are equally important in regulating C_{SAND} when $|\alpha| = 1$, changes in D_B are twice as important as changes in u_* in regulating C_{SAND} when $|\alpha| = 2$, and changes in u_* are twice as important as changes in D_B in regulating

C_{SAND} when $|\alpha| = 0.5$. By extension, changes in u_* completely control C_{SAND} as $|\alpha|$ approaches zero and changes in D_B completely control C_{SAND} as $|\alpha|$ approaches infinity. C_{SAND} is thus "flow regulated" when $|\alpha| < 1$ (because u_* is linearly related to both velocity and Q) and "grain-size regulated" when $|\alpha| > 1$. When $|\alpha| = 0$, sand transport is in equilibrium with the upstream sand supply and the bed-sand grain-size distribution does not change over time. In this situation, all of the sand delivered from upstream will pass through a river cross section without any change in bed-sand grain size such that the only regulator of C_{SAND} will be u_*, and stable relations between Q and C_{SAND} can be derived with zero variation about these relations. Therefore, equilibrium sand transport implies stationarity in sand-transport relations. As $|\alpha|$ increases, the degree of sand-transport disequilibria increases; at very large values of $|\alpha|$, changes in the upstream sand supply completely control sand transport by influencing bed-sand grain size.

We make the following approximation of Rubin and Topping (2001) so that equation (2) can be applied to an extensive data set (i.e., more than two cases):

$$\left|\frac{\log_{10}\Delta C_{SAND}}{\log_{10}\Delta D_S}\right| \approx \frac{\sigma(\log_{10}C_{SAND})}{\sigma(\log_{10}D_S)} \tag{3}$$

where σ indicates standard deviation. Because equation (3) calculates the absolute value but not the sign, the sign of $\log_{10}\Delta C_{SAND}/\log_{10}\Delta D_S$ is evaluated as the sign of the slope of $\log_{10}C_{SAND}$ regressed on $\log_{10}D_S$ when an F test indicates that this regression is significant and the correlation between $\log_{10}D_S$ and $\log_{10}C_{SAND}$ is moderate or stronger (i.e., $r > 0.4$). When this regression is insignificant or this correlation is weak, the sign of $\log_{10}\Delta C_{SAND}/\log_{10}\Delta D_S$ is indeterminate, and $|\alpha|$ is the mean $|\alpha|$ calculated using positive and negative $\sigma(\log_{10}C_{SAND})/\sigma(\log_{10}D_S)$ ratios.

3.5. Influence of Changes in β and α on "Relations" Between Discharge and Suspended-Sand Concentration and Between Discharge and the Sand Bedload Flux

When C_{SAND} is regulated by both u_* and bed-sand grain size, substantial systematic variation over time (i.e., hysteresis) in C_{SAND} will occur when C_{SAND} is plotted as a function of either only Q or bed-sand grain size. For example, decreasing bed-sand grain size, and therefore decreasing β, at constant Q or u_* will be associated with an increase in C_{SAND}. Large changes in bed-sand grain size (e.g., those associated with sand-wave passage) will thus result in increased $|\alpha|$ and variation about Q-C_{SAND} relations. Similarly, because the sand bedload flux (Q_{SB}) depends strongly on a flow parameter (typically the boundary shear stress) and bed-sand grain size (Einstein, 1950; Fernandez Luque & van Beek, 1976; Meyer-Peter & Müller, 1948; Schmeeckle & Nelson, 2003; van Rijn, 1984b; Wiberg & Smith, 1989; Wilcock & McArdell, 1993; Wilcock & Southard, 1989; Yalin, 1963), systematic variation in Q_{SB} will also occur when Q_{SB} is plotted as a function of only Q under conditions of changing bed-sand grain size.

We evaluated how changes in Q-C and Q-Q_{SB} relations reflected changes in β and how changes in the variation about Q-C_{SAND} relations reflected changes in α. "Relation" is used loosely in this context, owing to the large variation in C and Q_{SB} arising from the processes described above. For simplicity, we used a one-coefficient method to describe the mean Q-C and Q-Q_{SB} relations: least-squares linear regression forced through the origin. We then evaluated the strengths of the correlations between β and the slopes of the Q-C_{SAND} and Q-Q_{SB} relations and between log-transformed $|\alpha|$ and the mean sum of squares of the residuals about the Q-C_{SAND} relations. To reduce the influence of skewness on the correlation coefficient (r), the median was chosen in place of the mean to characterize the central tendency in β during each period. Similarly, because $|\alpha|$ is by definition highly right-skewed (i.e., it has a lower bound of zero and an upper bound of infinity), the log-transformed value of $|\alpha|$ was used to reduce the influence of skewness on r. These analyses were conducted at all five primary gaging stations for suspended sand, with data segregated into the same periods defined for the analyses of section 3.4. These analyses were conducted for bedload sand using slightly different periods (owing to fewer years of data) and at only the Yampa-Deerlodge station because only it has longer-term grain size-analyzed bedload data.

3.6. Sand Loads

We evaluated whether annual sand loads have changed over time and whether changes in loads have resulted from changes in β (i.e., bed-sand grain size), Q, or both. For the historical period at the stations

where the USGS published sediment loads (Table 1) and at the Vermillion Creek station, we subdivided loads into a silt and clay component and a sand component utilizing the sparser grain-size-analyzed EWI measurements (ranging from 0 to 40 measurements per year). For the 2012–2016 modern period, fluxes and cumulative loads were measured separately for silt and clay and for sand, so no post facto subdivision of loads into silt & clay and sand components was required.

Historical sand loads were estimated using two methods. (Method 1) *Sand rating curve*—where a stable relation was developed by regressing log-transformed C_{SAND} on log-transformed Q. This method was the less accurate of the two methods and was used only when the number of grain-size-analyzed EWI measurements per year was insufficient (i.e., $<$ ~9) to use Method 2, and the variance in C_{SAND} about the rating curve arising from likely systematic changes in bed-sand grain size was minimal. (Method 2) *Shifting sand rating curve*—where rating curves developed by Method 1 were allowed to shift over time. In this method, the ratio of EWI-measured to rating-curve-predicted C_{SAND} was first calculated at the time of each EWI measurement. Linear interpolation was then used to estimate these ratios for the days between these measurements. Multiplication of rating-curve-predicted values of C_{SAND} by these ratios thus resulted in rating-curve-predicted C_{SAND} that equaled EWI-measured C_{SAND}. The physical assumptions that justify this second method are described in Wright et al. (2010).

Because bedload rating curves that relate Q_{SB} to Q are likely to be dependent on bed-sand grain size, we developed an alternative approach to estimate Q_{SB} on the basis of the ratios of Q_{SB} to the suspended-sand flux (Q_{SS}) in paired bedload-EWI measurements. This approach consisted of log-transformed (Q_{SB}/Q_{SS}) regressed on log-transformed Q (Text S3). Because changing bed-sand grain size causes changes with identical sign in both Q_{SB} and Q_{SS}, this approach incorporated the effects of changing bed-sand grain size as captured by the suspended sand.

A 10% uncertainty was assigned to the 2012–2016 sand loads. The magnitude of this uncertainty results from the product of the likely maximum magnitudes of possible undetected, and therefore uncorrected, biases (i.e., systematic errors) in Q (e.g., Kiang et al., 2016; Sauer & Meyer, 1992) and C_{SAND} (e.g., Sabol & Topping, 2013; Topping et al., 2010) that may persist over long periods (Topping et al., 2010). Even though these possibly persistent biases are small relative to the random error in individual measurements of Q (Oberg & Mueller, 2007; Sauer & Meyer, 1992) and C_{SAND} (Topping & Wright, 2016; Topping et al., 2011, 2016), the absolute magnitudes of these biases accumulate over time because they are not random. This condition leads to an uncertainty that is expressed as a fixed percentage of the cumulative load. Because of greater potential bias in the methods used to estimate the historical sand loads, a 30% uncertainty was estimated for these loads. A 50% uncertainty was assigned to sand bedload on the basis of the likely maximum persistent bias in the Q-dependent relations used to estimate Q_{SB}.

3.7. Sand Budgets

We calculated sand budgets (with propagated uncertainty) to determine whether trends detected in the previous analyses were associated with river segments in sand surplus or deficit and whether sand-wave migration was greatly affected by longitudinal differences in channel geometry. Continuous mass-balance sand budgets were constructed for two parts of the study area: the "Deerlodge Park" and "Dinosaur" sediment-budget areas (Figure 1b). Input to the Deerlodge Park budget area was the combined 15-min sand flux at the Yampa-Maybell and LS-Lily stations; export from this budget area was the 15-min sand flux at the Yampa-Deerlodge station. Input to the Dinosaur budget area was the combined 15-min sand flux at the Green-Lodore and Yampa-Deerlodge stations; export from this budget area was the 15-min sediment flux at the Green-Jensen station. Sediment budgets could not be constructed pre-2012 owing to the lack of overlap in historical sediment-load record among gaging stations.

We also constructed a sand budget for the upper Green River between Flaming Gorge Dam and the Green-Lodore station to help evaluate the likelihood of dam-induced changes in bed-sand grain size (Figure 1a). This river segment has been interpreted to be in sediment deficit (Andrews, 1986; Schmidt & Wilcock, 2008) and sediment surplus (Grams & Schmidt, 2005). Input to this "Browns Park" budget was the water year 1972–1976 mean-annual sand load at the Red Creek station combined with the estimated mean-annual sand load of Vermillion Creek. The sand load of Vermillion Creek was estimated by assuming constant sand yield across this creek's drainage basin and then multiplying the 1976–1981 sand load at the Vermillion Creek

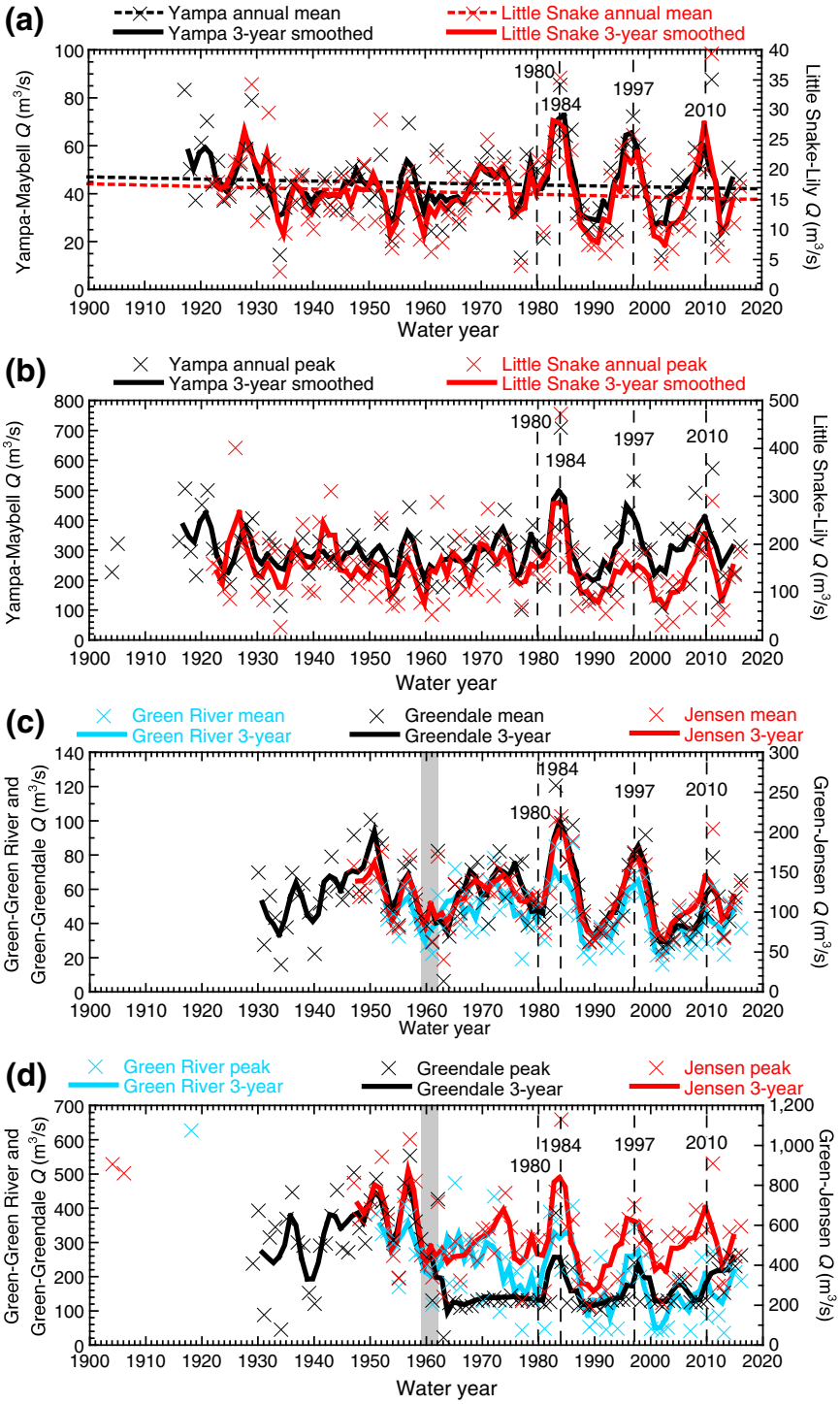

Figure 2. Raw and 3-year smoothed annual (a) mean and (b) peak *Q* at the Yampa-Maybell and LS-Lily stations and annual (c) mean and (d) peak *Q* at the Green-Green River, Green-Greendale, and Green-Jensen stations. Water year 1980 and peaks of post-1980 cycles described in text indicated by vertical dashed lines. Dashed lines in (a) are linear regressions indicating the minor (and insignificant) negative trends arising from the progressive increase in the consumptive use of water in the Yampa and Little Snake River basins (this use is now ~13% of the natural flow of these rivers). Gray-shaded boxes in (c) and (d) indicate the 1959–1962 construction period of Flaming Gorge Dam.

station by a factor of 4 to account for the drainage basin downstream from this station being ~3 times larger than the drainage basin upstream. Export from this budget was the mean-annual load computed from the water year 2013–2016 sand fluxes measured at the Green-Lodore station.

The contribution of sand from the small, ungaged tributaries was neglected in all sand budgets. Exclusion of this sand source thereby likely biased each budget slightly negative, but this bias is likely smaller than the magnitude of the propagated uncertainty associated with the measured sand input and export terms (Griffiths & Topping, 2017).

4. Results

4.1. Changes in Water Discharge

Long-term trends in *Q* in the Yampa and Little Snake rivers have been relatively slight and unlikely to greatly influence sand transport (Figures 2a and 2b and Text S7). The progressive increase in the consumptive use of water in these rivers (Colorado Water Conservation Board & Colorado's Decision Support Services, 2009a, 2009b) has resulted in slightly negative trends in annual mean *Q* that are statistically insignificant. Even though no significant long-term trends were detected, changes in the interannual *Q* variability have occurred that could affect sand transport. Three-year-smoothed time series (Figures 2a and 2b) suggest that the interannual variability in *Q* increased around 1980. This increase was associated with high-amplitude "cycles" of alternating wet and dry years coincident on both rivers. Manners et al. (2014) first recognized these wet-dry cycles in the Yampa River and their importance for vegetation-induced channel narrowing. The periodicity of these cycles was ~13 years, similar to the 9–12-year periodicity found by White et al. (2005) at stations on the Colorado and Snake rivers.

The detected changes in *Q* with the largest sand-transport implications have all occurred in the Green River as a result of Flaming Gorge Dam. Although dam operations have not significantly affected the annual mean *Q* of the upper Green River, they have reduced the mean-annual peak *Q* by ~50% (Figures 2c and 2d) and increased base flow. Because the Yampa River somewhat mitigates the effects of dam operations on *Q* in the middle Green River, the mean-annual peak *Q* at the Green-Jensen station decreased by only ~30%. While construction and operation of the dam has greatly changed peak and base flows in the upper Green River, it has not removed longer-term hydrologic cycles (cf. White et al., 2005) that potentially affect sand transport. Post-1980 cycles on the Yampa and Little Snake rivers also largely coincide with cycles in annual mean *Q* at the Green-Green River and Greendale stations, which bracket the dam.

4.2. Sources and Timing of Important Sand-Supplying Floods in Little Snake River Tributaries

Tributary floods that supply large amounts of sand to the Little Snake River are rare, and the largest of these floods have likely originated in Sand Creek. Field reconnaissance, inspection of aerial imagery, and analysis of the limited grain-size-analyzed suspended-sediment measurements made in these tributaries (U.S. Geological Survey, 2017d, 2017e, 2017f, 2017g, 2017h, 2017i) suggest that Sand Creek is a more important supplier of sand to the Little Snake River and that Muddy Creek primarily supplies silt and clay. Although floods have been documented in Muddy Creek, the analyses of streamflow records indicate that much larger floods likely occurred in Sand Creek.

Analyses of streamflow records from the Little Snake River indicate that the largest tributary floods have occurred in March in tributaries that enter the Little Snake River between the LS-Dixon and LS-Baggs stations (Figures 1 and 3a). Tributaries downstream from the LS-Baggs station only minimally affect *Q* at the LS-Lily station and are thus likely minor suppliers of sand. These results require that the detected large March floods occurred in either Muddy or Sand creeks. Comparison of Little Snake River and Muddy Creek streamflow records, however, indicates that these tributary floods had to mostly occur in Sand Creek. Analysis of the LS-Lily time series of March *Q* peaks indicates that the largest tributary floods occurred, in order of decreasing peak *Q*, in 1962, 1966, and 1956 (Figure 3b) and that the peak *Q* values of these floods greatly exceeded those of any documented Muddy Creek flood. No large tributary flood has occurred since 1966.

Precise determination that floods originated mostly in Sand Creek could be made for the 1962 and 1966 floods, when the Muddy-above Baggs peak-*Q* station and all three gaging stations on the Little Snake River were operating. During these floods, the daily mean *Q* values at the LS-Baggs and LS-Lily stations were similar but much larger than at the LS-Dixon station (Figure 4) and also much larger than the 1962 and 1966

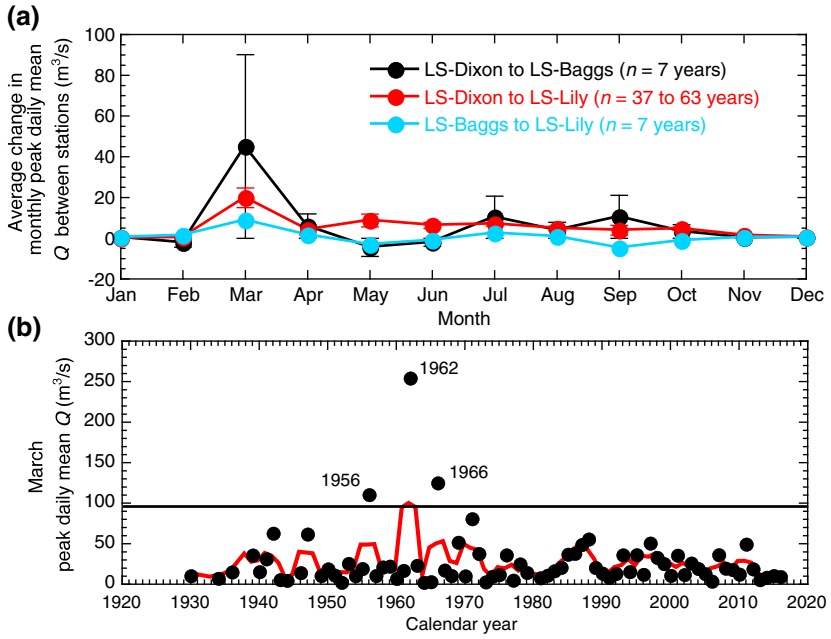

Figure 3. (a) Months and (b) years of large floods in tributaries to the Little Snake River. (a) Average change in monthly peak daily mean Q between the indicated gaging stations on the Little Snake River. Values calculated for the months during the years of overlap, n, where Q was reported on every day of the month. Error bars are one standard error. (b) Raw and 3-year smoothed (red line) peak daily mean Q at the LS-Lily station during March. Values shown are from floods with peaks distinct from the annual snowmelt flood; not all years have data because distinct peaks did not occur in all years. Black horizontal line indicates the chosen threshold associated with large tributary floods; this threshold Q is equal to the mean plus two standard deviations among the peak daily mean Q values. Years of tributary floods above this threshold are indicated.

peak instantaneous Q in Muddy Creek. Although less certain because it occurred 1.5 years before Muddy Creek was gaged, the 1956 flood also likely originated in Sand Creek because the daily mean Q associated with this flood at the LS-Lily station greatly exceeded the peak Q of the largest documented Muddy Creek flood.

4.3. Trends in β and Trends in Measured Bed-Sand Grain-Size Distributions

Significant time series trends in β were detected at all stations except on the upper Green River at the Green-Lodore station and on the upper Yampa River at the Yampa-Maybell station (Figure 5). These trends suggest a large-scale temporal pattern of fining of the sand on the beds of the Little Snake, lower Yampa, and Green rivers in the 1950s to mid-1960s, followed by bed-sand coarsening from the late 1960s to the present. Under constant or increasing Q, bed-sand fining (decreasing β) indicates an increasing upstream sand supply, whereas under constant or decreasing Q, bed-sand coarsening (increasing β) indicates a decreasing upstream sand supply (Topping et al., 2000). Changes in Q can be ruled out as the cause of the observed pattern of grain-size change. No net change in Q occurred during the periods of grain-size change in the Little Snake and lower Yampa rivers (Figures 2a and 2b). Furthermore, no net change in Q occurred in the Green River during the period of bed-sand fining that began before closure of Flaming Gorge Dam, and Q did not increase during the post-1960s period of bed-sand coarsening in the middle Green River (Figures 2c and 2d). The regional pattern of grain-size change suggests that sand was delivered to the channel network throughout most of the study area at a much greater rate in the mid-20th century and that the supply of sand has been much less thereafter.

Bed-sand fining in much of the study area ended in the mid-1960s. Between 1951 and the 1964 completion of Fontenelle Dam, β significantly decreased at the Green-Green River station (Figure 5a). Flaming Gorge Dam was thus constructed during a period of bed-sand fining in the upper Green River. A similar temporal pattern of fining occurred in the Little Snake River, where the greater spatial resolution of gaging stations indicates that the likely source of the increased sand supply causing the fining was Sand Creek. β significantly decreased (p = 0.024) between 1958 and 1963 at the LS-Lily station on the Little Snake River (Figure 5d),

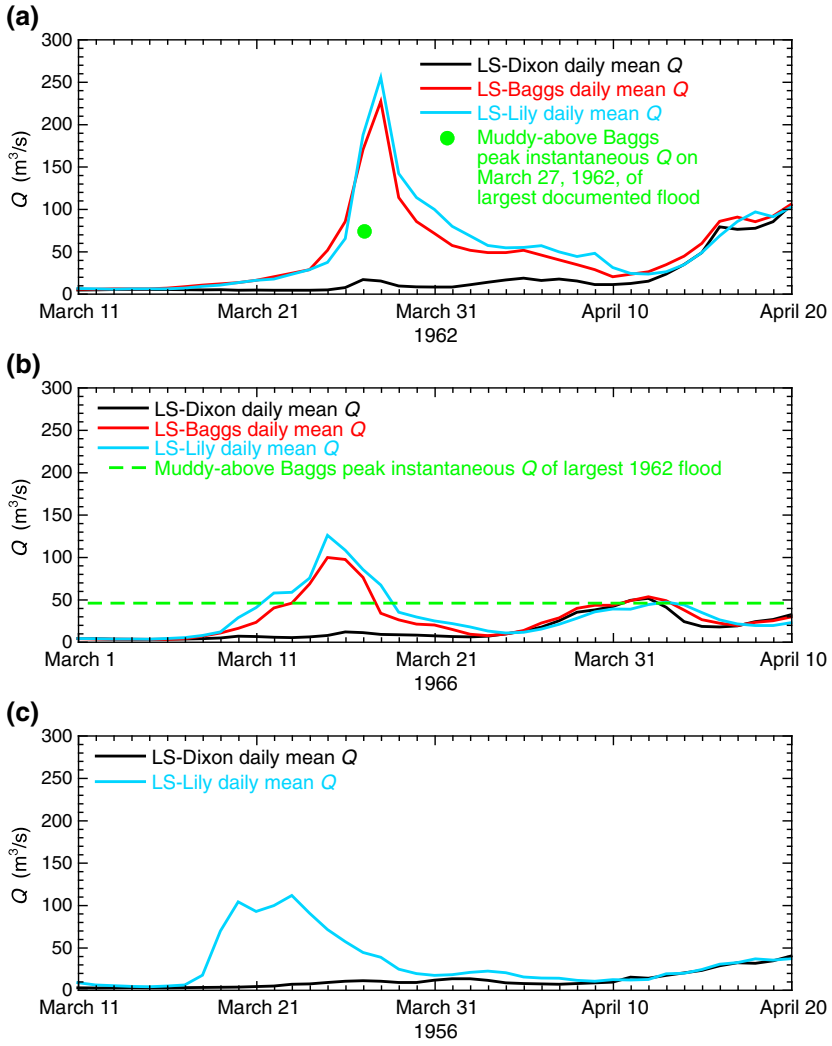

Figure 4. Daily mean *Q* at the LS-Dixon, LS-Baggs, and LS-Lily stations during the (a) March 1962 and (b) March 1966 Sand Creek floods, and likely (c) March 1956 Sand Creek flood. Also shown in (a) is the 27 March 1962 peak instantaneous *Q* of the largest documented flood on Muddy Creek (Text S5). Dashed line in (b) indicates the value of the peak instantaneous *Q* during the largest 1966 flood on Muddy Creek (reported to have occurred on May 11).

with much of this decrease occurring immediately after the largest Sand Creek flood that peaked on 28 March 1962. As a likely consequence of this tributary flood, the annual mean value of β at the LS-Lily station decreased from 1.04 in 1961 to 0.72 in 1962. β also significantly decreased ($p = 0.0049$) between 1951 and 1965 at the Green-Jensen station downstream from the confluence of the upper Green and Yampa rivers, with the largest and most rapid decrease in β during this period also occurring immediately after the 1962 Sand Creek flood (Figure 5f). Consequently, the annual mean value of β at the Green-Jensen station decreased from 1.17 in 1961 to 0.82 in 1962 after the Sand Creek flood. This rapid decrease in β in the middle Green River at the Green-Jensen station is the likely result of the downstream propagation of bed-sand fining from the Little Snake River because ongoing construction of Flaming Gorge Dam had already begun disrupting the upstream sand supply to the upper Green River by 1962.

β progressively increased at the LS-Lily, Yampa-Deerlodge, and Green-Jensen stations after the mid-1960s, indicating net coarsening of the bed sand throughout most of the study area caused by a decrease in the rate of sand supplied to the river network. Although it is impossible to determine exactly when β began increasing at the LS-Lily station owing to a 1965–1977 data gap, it is likely that the bed sand in the Little Snake River began coarsening by the late 1960s, because no large floods on upstream tributaries have occurred since

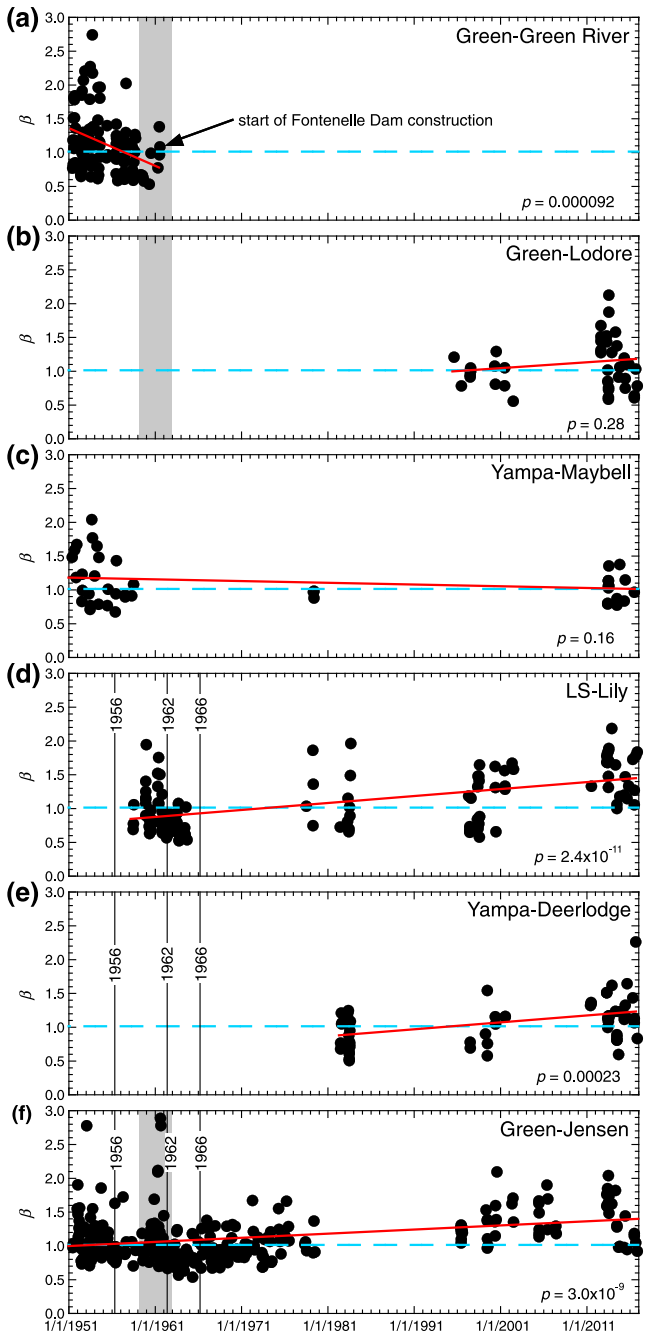

Figure 5. β time series at the following stations: (a) Green-Green River, (b) Green-Lodore, (c), Yampa-Maybell, (d) LS-Lily, (e) Yampa-Deerlodge, and (f) Green-Jensen. Solid red line is the least-squares linear regression fit to β for the entire period of record; significance, p, of these regressions is indicated. Horizontal blue dashed lines indicate $\beta = 1$. Gray shaded boxes in (a), (b), and (f) indicate construction period of Flaming Gorge Dam. Solid black vertical lines labeled "1956," "1962," and "1966" in (d) through (f) indicate the dates of large sand-supplying floods in the Little Snake River tributary Sand Creek (located upstream from these stations). Of these three floods, the March 1962 flood had, by far, the largest peak Q and therefore likely supplied the largest amount of sand to the Little Snake River.

15 March 1966. Although no pre-1982 data exist at the Yampa-Deerlodge station (Figure 5e), it is likely that bed-sand coarsening in the lower Yampa River also began in the late 1960s, because this station is located between the LS-Lily and Green-Jensen stations, and most of the sand in the lower Yampa River is supplied by the Little Snake River. Coarsening of the bed sand at the Green-Jensen station began between 1965 and 1973, and β values <0.9 have not reoccurred since 1975.

The long-term changes in β in Figure 5 reflect changes mainly in the fine tail of the bed-sand grain-size distribution (Figure 6), because of the relative coarseness of the bed sand in the study area (i.e., high Rouse numbers). At the Green-Lodore station, although short-term variation is present, there was no net change in β between 1995 and 2016, and no net change in the measured bed-sand grain size between 1982 and 2016 (Figure 6a). Between 1982 and 2016 at the LS-Lily and Yampa-Deerlodge stations, β increased as the measured bed-sand grain-size distribution coarsened predominantly through winnowing (Figures 6b and 6c). As a result of this winnowing process (e.g., Rubin et al., 1998), only bed-sand D_{02} increased significantly at these stations, with no significant change in D_{05}, D_{10}, D_{16}, or D_{50}.

4.4. α Analyses

α-analysis results indicate that sand transport in the study area is generally in disequilibrium with the upstream sand supply, with changes in the upstream sand supply partially to fully regulating C_{SAND} through changes in bed-sand grain size. Although $|\alpha|$ values near unity indicate that changes in Q and changes in bed-sand grain size were roughly equal in regulating C_{SAND} in most of the study area over longer timescales, there are periods of elevated $|\alpha|$ that indicate that changes in bed-sand grain size controlled sand transport during discrete periods in the Little Snake and middle Green rivers (Figure 7 and Text S8). Only at the Green-Greendale station in 1958 was sand transport in quasi-equilibrium with the upstream sand supply, as evidenced by near-zero $|\alpha|$. The subsequent large increase in $|\alpha|$, from 0.016 at this station to 0.92 in 1995–2016 at the Green-Lodore station, suggests that closure of Flaming Gorge Dam greatly increased the importance of changes in bed-sand grain size in regulating C_{SAND} in the upper Green River. This increase in grain-size regulation likely arises from the reduction of the upstream sand supply and greater postdam importance of Red and Vermillion creeks as the suppliers of sand to the upper Green River, with episodic bed-sand fining from resupply of sand from these tributaries interspersed with bed-sand winnowing during periods of tributary quiescence (as evidenced by the short-term variation in β in Figure 5b).

Not surprisingly, grain-size regulation of C_{SAND} dominates during periods of rapid change in the upstream sand supply, and flow (i.e., Q) regulation of C_{SAND} dominates during periods of sustained elevated or reduced sand supply. Thus, the two largest increases in $|\alpha|$ in the study area occurred in the Little Snake and middle Green rivers as the result of the bed-sand fining following large Sand Creek floods (Figures 5d–5f). Although changes in bed-sand grain size were already important for regulating C_{SAND} in the Little Snake River (possibly as the result of the likely 1956 Sand Creek flood), $|\alpha|$ increased from 1.08 to 6,010 at the LS-Lily station following the largest Sand Creek flood that peaked on 28 March 1962 (Figure 7c). Downstream propagation of the bed-sand fining caused by the Sand

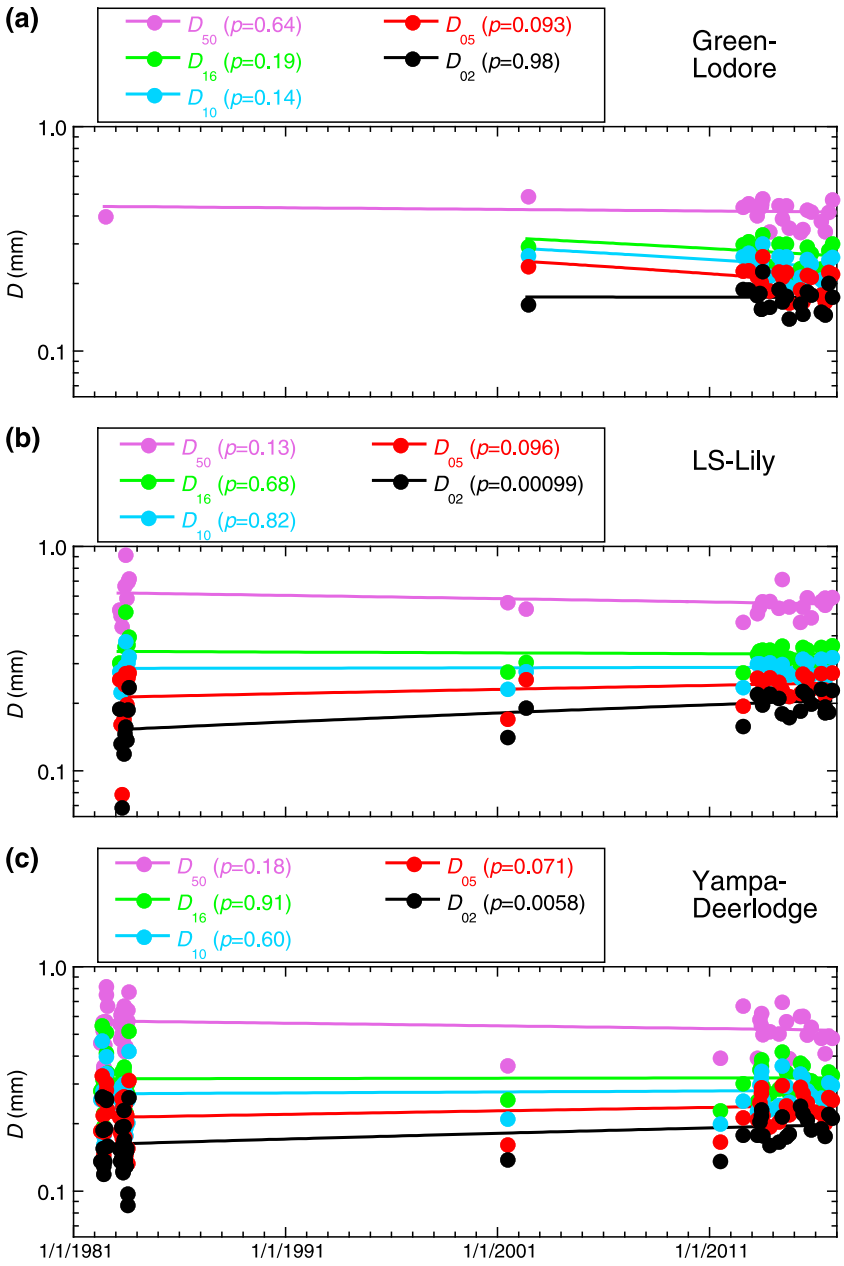

Figure 6. Time series of bed-sand D_{02}, D_{05}, D_{10}, D_{16}, and D_{50} at the following stations: (a) Green-Lodore, (b) LS-Lily, and (c) Yampa-Deerlodge. Solid lines are the least-squares linear regressions fit to β for the entire period of record, with significance, p, of these regressions indicated in the legend. No other grain-size metrics from the 1982 measurement of Andrews (1986) could be included in (a) because he reported only the D_{50}.

Creek flood(s) transformed the middle Green River from a river in which C_{SAND} was regulated mostly by changes in Q to one in which C_{SAND} was almost equally regulated by changes in Q and bed-sand grain size. $|\alpha|$ thus increased from 0.478 to 0.747 at the Green-Jensen station between the 1951–1958 and 1959–1964 periods (Figure 7e). The other large increase in $|\alpha|$ (from 0.691 to 1.30) in the study area occurred at the Green-Jensen station as the bed sand coarsened after 1973 (Figures 5f and 7e).

4.5. Associated Changes Between β, α, and Q-C_{SAND} and Q-Q_{SB} Relations

The results described in the preceding sections demonstrate that sand supplied from Sand Creek during an extremely large flood in 1962 caused the bed of the Little Snake River to fine (β decreased). Associated with

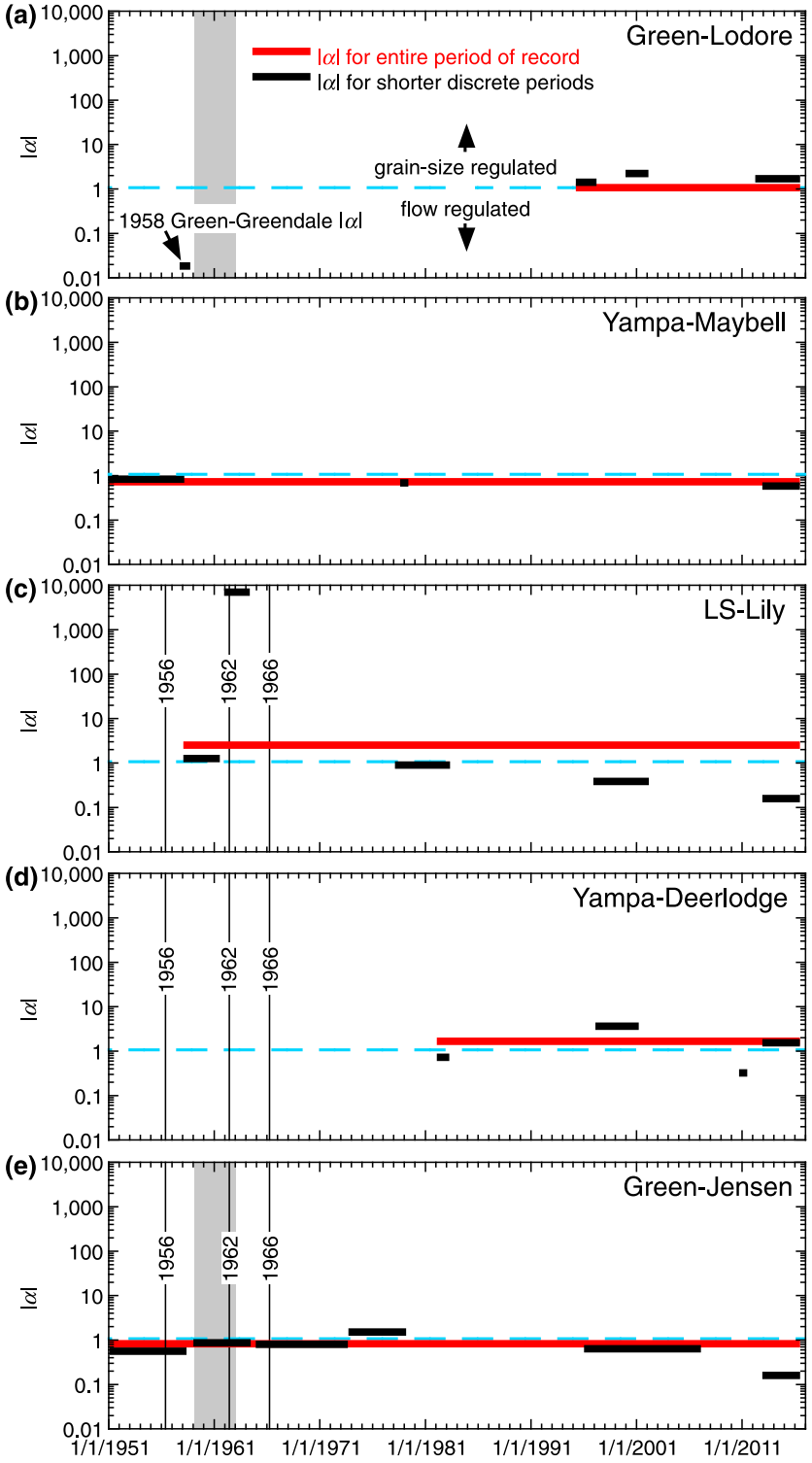

Figure 7. $|\alpha|$ at the following stations: (a) Green-Lodore (with Green-Greendale for pre-dam context), (b) Yampa-Maybell, (c) LS-Lily, (d) Yampa-Deerlodge, and (e) Green-Jensen. The extents of the heavy horizontal red and black lines indicate the periods over which $|\alpha|$ was computed. Horizontal blue dashed lines indicate $|\alpha| = 1$, the value at which changes in the bed-sand grain size and flow are equally important in regulating C_{SAND}. Gray shaded boxes in (a) and (e) indicate construction period of Flaming Gorge Dam. Solid black vertical lines labeled "1956," "1962," and "1966" in (c) through (e) indicate the dates of large sand-supplying floods in the Little Snake River tributary Sand Creek (located upstream from these three stations). Of these three floods, the March 1962 flood had, by far, the largest peak Q and therefore likely supplied the largest amount of sand to the Little Snake River.

Table 2
Median β and Slopes of Q-C and Q-Q_{SB} Relations for Total Sand and Sand in Four Size Classes (Very Fine, Fine, Medium, and Coarse Sand) at Each Station (in Bold) During Discrete Periods; r Value Next to Each Station Name Indicates the Strength of the Correlation Between the Median β Values and the Slopes of the Q-C_{SAND} or Total-Sand Q-Q_{SB} Relations Among the Discrete Periods

			Slope of *Q-C* relation				
Water years	*n*	Median β	Total sand	Very fine sand	Fine sand	Medium sand	Coarse sand
Green-Greendale							
1958	16	1.10	1.36	0.52	0.55	0.27	0.005
Green-Lodore ($r = -0.97$)							
1995–1997	7	1.01	0.60	0.14	0.31	0.14	0.009
2000–2002	6	0.939	0.81	0.30	0.29	0.22	0.000
2012–2016	32	1.12	0.46	0.18	0.21	0.06	0.005
Yampa-Maybell ($r = -0.78$)							
1951–1958	27	1.02	0.19	0.11	0.048	0.030	0.003
1976–1979	4	0.978	0.42	0.20	0.21	0.012	0.000
2013–2016	23	1.05	0.25	0.14	0.084	0.025	0.001
LS-Lily ($r = -0.86$)							
1958–1961	64	0.864	11.13	5.29	3.63	1.85	0.37
1962–1964	61	0.723	11.88	7.17	3.34	1.23	0.13
1978–1983	14	1.03	7.18	3.10	2.27	1.06	0.75
1994–2002	32	1.16	3.41	1.70	1.03	0.56	0.12
2011	1	1.34	---	---	---	---	---
2013–2016	24	1.67	3.33	0.96	1.36	0.84	0.16
Yampa-Deerlodge ($r = -0.98$)							
1982–1983	21	0.889	0.95	0.49	0.26	0.17	0.038
1994–2001	12	0.984	0.73	0.32	0.23	0.13	0.035
2011	3	1.36	0.25	0.054	0.084	0.078	0.038
2013–2016	27	1.14	0.47	0.16	0.19	0.09	0.024
Green-Jensen ($r = -0.84$)							
1951–1958	82	1.04	1.26	0.52	0.48	0.20	0.054
1959–1964	100	0.895	1.65	0.78	0.64	0.23	0.012
1965–1973	74	0.921	1.50	0.78	0.54	0.17	0.012
1974–1979	26	1.08	0.62	0.20	0.24	0.19	0.017
1996–2007	42	1.30	0.80	0.31	0.37	0.12	0.003
2013–2016	25	1.49	0.54	0.14	0.20	0.16	0.042
			Slope of *Q*-Q_{SB} relation				
			Total sand	Very fine sand	Fine sand	Medium sand	Coarse sand
Yampa-Deerlodge ($r = -1.0$)							
1982–1983	31	0.889	0.038	0.00021	0.0017	0.015	0.017
1998–2001	22	1.11	0.029	8.9×10^{-6}	0.00071	0.0088	0.012

Note. n indicates the number of EWI or bedload measurements in each period.

this bed-sand fining, C_{SAND} became dominantly grain-size regulated ($|\alpha|$ increased). Subsequently, these patterns in β and $|\alpha|$ propagated downstream, and we documented similar patterns in the middle Green River at the Green-Jensen station downstream from the confluence of the Yampa and upper Green Rivers. Thereafter, the bed sands of the study area coarsened because there were no more large deliveries of sand to the Little Snake River from Sand Creek after 1966. At the same time, the flow regime of the Green River part of the study area also changed as a result of Flaming Gorge Dam operations.

Changes in β infer changes in bed-sand grain size, and these inferences are consistent with the bed-sediment measurements. Because bed-sand grain size is an important regulator of suspended and bedload sand, it is not surprising that there were systematic shifts in *Q*-C_{SAND} and *Q*-Q_{SB} relations that coincided with the β-inferred changes in bed-sand grain size. These relations shifted upward, with increases in slope, when the bed sand fined (i.e., β decreased) and shifted downward, with decreases in slope, when the bed sand coarsened (Table 2). The correlations between β and the slopes of these relations are, as expected, all negative and are

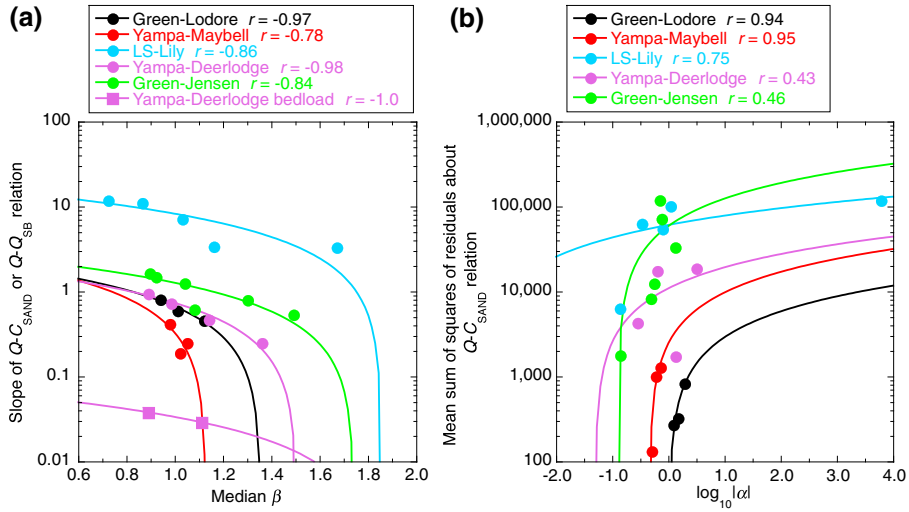

Figure 8. (a) Slope of the Q-C_{SAND} or total-sand Q-Q_{SB} relation plotted as a function median β and (b) the mean sum of squares of the residuals about the Q-C_{SAND} relation plotted as a function of log-transformed $|\alpha|$ during each discrete period at the five primary gaging stations. Periods listed in Table 2. r values in the legends are the correlation coefficients associated with the least-squares linear regressions (solid lines) depicted in each figure panel. The slope of the Q-Q_{SB} relation for total sand could be plotted as a function of median β at only the Yampa-Deerlodge station because sufficient sand bedload measurements existed at only that station.

generally very strong to nearly perfect, with r values ranging from −0.8 to essentially −1.0 (Table 2 and Figure 8a). During periods of relatively rapid change in β, grain-size regulation of C_{SAND} became more important with increased values of $|\alpha|$ and, as expected, increased variation in C_{SAND} about the Q-C_{SAND} relations. Thus, correlations between log-transformed $|\alpha|$ and the mean sum of squares of the residuals about these relations are positive and generally moderate to very strong, with r values ranging from 0.4 to 0.9 (Figure 8b).

Regardless of the direction of the change in β, the coincident changes in the C and grain-size distribution of the suspended sand are manifest primarily by changes in the C of the finer size classes of sand, with progressively lesser change in the C of the coarser size classes. Similarly, post-1982 bed-sand coarsening at the Yampa-Deerlodge station was also associated with downward shifts in the Q-Q_{SB} relations that were progressively and relatively larger for the finer size classes of sand. Plots showing the temporal changes in the relations between Q and C_{SAND}, D_{50}, and C for four size classes of suspended sand are in Text S9. These plots also show the temporal changes in the variation in C_{SAND} about the Q-C_{SAND} relations. Consistent with the β and α analyses, the largest changes in the Q-C_{SAND} relations and suspended-sand D_{50} occurred at the LS-Lily, Yampa-Deerlodge, and Green-Jensen stations.

4.6. Influence of Flaming Gorge Dam on Bed-Sand Grain Size in the Upper Green River

Although there have been no net changes in bed-sand grain size at the Green-Lodore station since at least 1982, a lack of any older data at this station makes it impossible to know whether closure of Flaming Gorge Dam caused coarsening of the bed sand in this part of the upper Green River between 1962 and 1982. Comparison of Q-C relations between the Green-Greendale and Green-Lodore stations was therefore used to determine whether early postdam coarsening of the bed sand at the Green-Lodore station was likely, merely possible, or unlikely. Though there are no overlapping predam sediment-transport measurements at the Green-Greendale and Green-Lodore stations, we postulate that the predam sand loads at these stations were approximately similar because the intervening tributary sand supply is very small compared to the predam sand load at the Green-Greendale station (Text S10). We therefore assume that the predam Q-C_{SAND} relations at these stations were also similar, thus allowing application of predam Green-Greendale Q-C relations at the Green-Lodore station. This operation suggests that the Q-C relations at the Green-Lodore station for total suspended sand, very fine sand, and fine sand may have shifted downward between 1958 and 1995 (Table 2 and Text S9), with little change in the relations for medium and coarse sand. Because these possible shifts would have been larger for the finer size classes, the bed sand at the Green-Lodore station could have

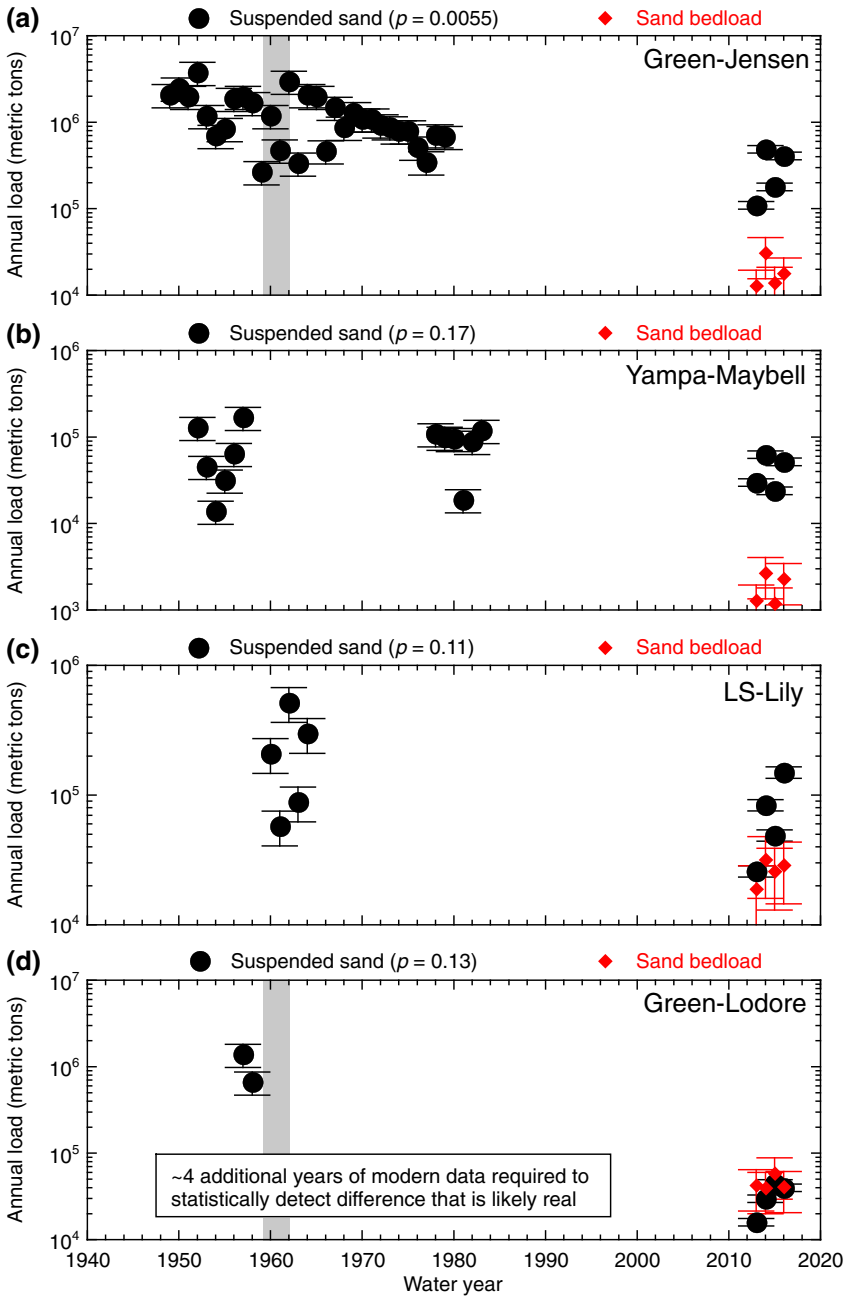

Figure 9. Annual suspended-sand load and sand bedload during each water year at the (a) Green-Jensen, (b) Yampa-Maybell, (c) LS-Lily, and (d) Green-Lodore stations. Error bars are the uncertainties described in section 3.6; *p* values from WMW tests comparing the historical and 2013–2016 loads. 1957–1958 loads in (d) are from the Green-Greendale station. Gray shaded boxes in (a) and (d) indicate construction period of Flaming Gorge Dam.

been finer predam than during 1982–2016, though this cannot be known for certain. Therefore, because it is not possible to know whether Flaming Gorge Dam caused bed-sand coarsening at the Green-Lodore station before 1982, it remains unclear as to whether any of the post-1965 bed-sand coarsening downstream at the Green-Jensen station was caused by the dam.

4.7. Sand Loads

Temporal changes in annual sand loads generally support the results from the analyses of changes in Q and β, with a few exceptions owing to sparse annual-load data (Figure 9 and Text S10). This result indicates that the

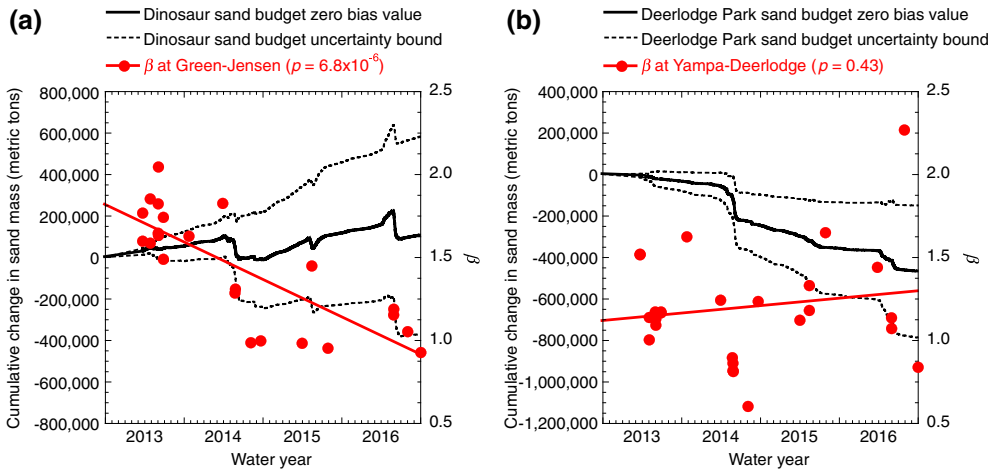

Figure 10. Comparison of the continuous mass-balance sand budgets and β calculated from the EWI measurements made at the downstream gaging station for the (a) Dinosaur and (b) Deerlodge Park budget areas. Shown are the "zero bias values," that is, the sand budgets calculated without any uncertainty, and the upper and lower uncertainty bounds. Budgets use estimated loads before continuous suspended-sand measurements began in late October 2012 at the Green-Lodore and Yampa-Deerlodge stations and in mid-March 2013 at the Yampa-Maybell, LS-Lily, and Green-Jensen stations (Text S10). β calculated using the reference values for the entire period of record at each station (not just water years 2013–2016). Solid red lines are least-squares linear regressions fit to 2013–2016 β values; p values are from the F tests conducted on these regressions.

analyses presented in the previous sections are more sensitive to detecting changes in sand transport than are statistical analyses of relatively few years of sand-load data. At the one station where a decrease in peak Q and increase in β have occurred, that is, the Green-Jensen station, significant decreases in annual suspended-sand loads were detected between the historical and 2013–2016 periods (Figure 9a), with these decreases beginning during the historical period upon closure of Flaming Gorge Dam. At the Yampa-Maybell station, where no significant net change in Q or β occurred over time, no significant difference between historical and 2013–2016 suspended-sand loads was detected (Figure 9b). However, owing to the small number of years with data, no statistically significant difference existed between the historical and 2013–2016 suspended-sand loads at the LS-Lily station (Figure 9c) despite large increases in β and associated downward shifts in the Q-C_{SAND} relations (Figure 5d and Table 2). Similarly, even though it graphically appears (and is extremely likely) that major decreases in the suspended-sand loads (Figure 9d) occurred at the Green-Lodore station between 1958 and 2013, there are insufficient data to detect these decreases using WMW tests.

4.8. Sand Budgets

4.8.1. Deerlodge Park and Dinosaur Continuous Mass-Balance Sand Budgets and β

The sand budgets indicate substantial differences in the patterns of sand deposition and erosion between the Deerlodge Park and Dinosaur sediment-budget areas (Figures 1b and 10 and Table 3). In the Deerlodge Park budget area, net erosion of sand occurred during the entire water year 2013–2016 period and during each of the individual water years. Although no net demonstrable change in sand mass occurred in the Dinosaur budget area, net deposition of sand likely occurred in water year 2013 and definitely occurred in water year 2015. These years were lower-Q years, with peak $Q < 450$ m^3/s. The sign of the Dinosaur sand budget during the two higher-Q years was indeterminate.

In sand-bedded rivers without bed armoring, net accumulation of sand is generally associated with bed-sand fining, and net erosion of sand is generally associated with bed-sand coarsening (winnowing) (Topping et al., 2000; Wright et al., 2010). The degree of bed-sand fining or coarsening depends on the volume of sand in the bed and banks and the thickness of the active layer (Bennett & Nordin, 1977; Parker, 2008). Thus, the sign of a sand budget and the sign of β at the downstream gaging station will likely be negatively correlated, although there may be a lag between the response of a sand budget and β depending on the longitudinal distance between the locations of large changes in sand storage and the downstream gaging station.

Table 3
Changes in Sand Mass in Metric Tons, With Propagated Uncertainty, in the Deerlodge Park and Dinosaur Sediment-Budget Areas[a]

	Deerlodge Park budget area		Dinosaur budget area	
Water years	Change in sand mass	Budget status	Change in sand mass	Budget status
2013–2016[b]	−470,000 ± 320,000	negative	100,000 ± 480,000	indeterminate
2013[b]	−36,000 ± 44,000	likely negative	49,000 ± 69,000	likely positive
2014	−210,000 ± 100,000	negative	−59,000 ± 160,000	indeterminate
2015	−110,000 ± 75,000	negative	120,000 ± 110,000	positive
2016	−110,000 ± 95,000	negative	−10,000 ± 130,000	indeterminate

[a]Budgets are indeterminate when the uncertainty is ≥2 times the absolute value of the zero-bias value; budgets are demonstrably positive or negative when the uncertainty is < the absolute value of the zero-bias value; budgets are likely positive or negative when the uncertainty falls between these bounds. [b]Values in this row include the estimated October 2012 loads at the Green-Lodore and Yampa-Deerlodge stations and the estimated October 2012 to early March 2013 loads at the Yampa-Maybell, LS-Lily, and Green-Jensen stations (Text S10).

In the case of the Dinosaur sand budget, the sign of this budget during much of 2013–2016 was positive, whereas the slope of the trend in β was strongly (and significantly) negative (Figure 10a). In the case of the Deerlodge Park sand budget, the sign of the budget was negative, whereas the slope of the trend in β was only weakly (and insignificantly) positive (Figure 10b). The weaker negative correlation between the signs of the sand budget and β in the Deerlodge Park case suggests that either the active layer is thicker (thus causing bed-sand grain size to change more slowly) than in the Dinosaur budget area or perhaps the "true" location of the budget is closer to the upper uncertainty bound than the zero bias values (owing to the possible influence of neglected sand from ungaged tributaries).

4.8.2. Estimated Sand Budget for Browns Park

Based on historical measurements from the 1970s and 1980s, the estimated mean-annual sand supply to the segment of the upper Green River in Browns Park from Red and Vermillion creeks is 34,000 ± 10,000 metric tons. Given that all stations in our study area show either no net change or a net decrease in sand transport between the 1960s and 2013–2016, it is unlikely that this is an underestimate of the sand supply from these tributaries. During water years 2013 through 2016, the mean-annual sand export from Browns Park past the Green-Lodore station was 79,000 ± 26,000 metric tons. Given the uncertainties, between a factor of 1.2 and 4.4 more sand was therefore exported from this river segment during 2013–2016 than was likely supplied to it. In addition, between 21 and 64% of this sand export occurred during only the four spring floods released from Flaming Gorge Dam in this period. Our measurements therefore suggest that the long-term mean-annual sand budget for Browns Park is negative, consistent with the conditions that would cause the possible postdam coarsening of the bed sand at the Green-Lodore station inferred in section 4.6.

5. Discussion

5.1. Sand Wave Conceptual Model for Sand Transport Through the Study Area

Sand transport is generally in disequilibrium with the upstream sand supply in the study area and is governed by episodic tributary resupply of large amounts of sand and changes in water discharge. Under natural conditions, as in the Little Snake and lower Yampa rivers, pulses of sand from tributaries propagate downstream, affecting bed-sand grain size and sand transport. These coupled changes in sand grain size and transport propagate downstream into more distal river segments, as indicated in the middle Green River at the Green-Jensen station.

The conceptual model governing the natural downstream transport of sand and finer sediment in the study area is nearly identical to the sand-wave model described by Topping et al. (2000) for the Colorado River downstream from Glen Canyon Dam. During a large tributary flood, large amounts of sand are supplied to the main-stem channel. In the case of the Little Snake River, the tributary is Sand Creek; in the case of the lower Yampa River, the tributary is the Little Snake River; and, in the case of the middle Green River, the tributary is the Yampa River. Because its amount is finite, is episodically supplied to the river, and is finer than the bed sand, the sand supplied during a tributary flood will result in the initiation of a sand wave in the river, with a component of this wave in the suspended load, the bedload, and in the bed itself. Owing to their lower

settling velocities and therefore lower Rouse numbers, the finer size classes in this sand wave will be carried higher in the water column where velocities are higher and thus be carried downstream at progressively higher velocities.

As a sand wave travels downstream, it will elongate, with the finest size classes outrunning the coarser size classes, thus causing substantial changes to the grain-size distribution of the bed (e.g., Topping et al., 2000, 2007). When the dominant transport mode is suspension, the principal equations and parameters that govern the downstream migration of a sand wave and the exchange of sand between suspension and the bed are the 2-D version of the suspended-sediment advection-diffusion equation for individual size classes of sand:

$$\frac{\partial \overline{C}_m}{\partial t} + \frac{\partial \left(\overline{u}\overline{C}_m\right)}{\partial x} - \partial\left(\overline{C}_m\left(1 - \sum_{m=1}^{M}\overline{C}_m \text{ww}_m\right)\right)/\partial z = \frac{\partial}{\partial x}\left(2K(z)\frac{\partial \overline{C}_m}{\partial x}\right) + \frac{\partial}{\partial z}\left(K(z)\frac{\partial \overline{C}_m}{\partial z}\right) \tag{4}$$

the flux lower boundary condition for suspended sand (Parker, 1978; Topping et al., 2007):

$$K(z)\frac{\partial \overline{C}_m}{\partial z} = \left(\overline{C}_m\right)_a\left(\sum_{m=1}^{M}\overline{C}_m \text{ww}_m - \text{ww}_m\right) \tag{5}$$

the thickness of the active layer (Bennett & Nordin, 1977; Parker, 2008), and the multi-size-class conservation of mass relation between the bed sand in the active layer and the sand in transport (Exner, 1920, 1925; Ferguson et al., 2015; Parker, 2008). In equations (4) and (5), x is the downstream dimension and z is the vertical dimension, $\overline{C}_m$ is the time-averaged concentration of sand in individual size-class m (of M total size classes), $\overline{u}$ is the time-averaged downstream component of velocity, ww_m is the settling velocity of sand in size-class m, $K(z)$ is the eddy viscosity, and $\left(\overline{C}_m\right)_a$ is the time-averaged reference concentration of sand in size-class m at elevation a near the bed (McLean, 1992; Topping et al., 2007). Equations (4) and (5) must be solved for all M size classes of sand. The 2 in the first term on the right side of equation (4) is an approximation that arises from the measurements of Fischer (1973). The downstream migration of a sand wave depends on the amount and grain-size distribution of tributary-supplied sand relative to the antecedent thickness and grain-size distribution of the riverbed sand under varying flow conditions. By the physics described by equations (4) and (5), the rate of sand-wave migration, and therefore the rate of fining and subsequent bed-sand coarsening associated with the passage of a sand wave depends on the upstream sand supply, the thickness of the bed-sand active layer, the mass conservation between each size class of sand in the active layer and in transport, the boundary shear stress (both total and skin-friction), the flow depth, velocity profile, and bed roughness. Many of these quantities are imprecisely known or unknown in the study area. Numerical solution of a sand-wave model requires adequately knowing all of these quantities, solving equations (4) and (5) over all M size classes of sand, and solving for the evolving bed-sand grain-size distribution in the active layer. Thus, we provide only a qualitative description of the physical implications of equations (4) and (5).

Owing to equations (4) and (5), and mass conservation of sand between suspension and the active layer, the arrival of a sand wave will result in the condition where the upstream sand supply is enriched and the amount of finer sand in suspension exceeds that which can be supported over the coarser antecedent grain-size distribution of the bed (a condition typically referred to as overloading). This process results in a mass transfer of the progressively finer size classes in suspension to the bed, causing fining of the bed sand. The amount and rate of change in the bed-sand grain-size distribution depends on (4) and (5), and the thickness of the active layer. As the bed fines (and β decreases), progressively more finer sand can be suspended, resulting in an increase in C_{SAND} and a decrease in the D_{50} of the suspended sand without any change in Q (e.g., the herein presented upward shifts in Q-C_{SAND} relations). Because the arrival of a sand wave results in an increase in C_{SAND} associated with a decrease in D_{50} in both the suspended and bed sand, with no change in Q, this arrival can be detected as a large increase in $|\alpha|$. Then, as the fine leading edge of the sand wave passes downstream, a reverse mass transfer occurs. As the concentration of the finer sand size classes in suspension decreases below that which can be supported by the grain-size distribution of the bed (a condition typically referred to as underloading), the bed is winnowed and the finest size classes in the bed are transferred back into suspension, resulting in progressive coarsening of the bed sand (and increase in β). Thus, in the tail of the sand

wave, C_{SAND} decreases as the D_{50} of the suspended sand increases, again, without any change in Q (e.g., the downward shifts in Q-C_{SAND} relations). As this occurs, C_{SAND} becomes progressively more regulated by changes in Q (e.g., the gradual decreases in $|\alpha|$ at the LS-Lily and Green-Jensen stations). Depending on the influence of a sand wave on transport (i.e., the magnitude of bed fining and increased sand transport associated with the downstream migration of the leading edge), there may not be much of a topographic signature of a sand wave. For example, Ferguson et al. (2015) demonstrated that a sediment wave migrating over a coarser riverbed could result in relatively little bed elevation change because increases and decreases in transport can be accommodated by fining and coarsening of the riverbed. Flume studies of gravel-bed streams have similarly shown that finer sediment pulses have higher wave celerities (Sklar et al., 2009) and can produce a dramatic change in surface grain size that drives increased sediment transport (Venditti et al., 2010).

In the case of the Colorado River in Grand Canyon, these same sand-wave processes propagate downstream with a relatively high celerity such that the episodes of bed fining followed by coarsening back to the antecedent bed condition can occur within 1 year in a 100-km-long river segment (Topping et al., 2000). Our present study suggests, however, that this process can operate over many decades when there are few large sand-supplying tributary floods. In the case of the Little Snake River, although the rapid decrease in β and rapid increase in $|\alpha|$ following the extremely large Sand Creek flood of 28 March 1962 suggests that the fine leading edge of a sand wave may transit the entire ~117-km-long river segment between Sand Creek and the LS-Lily station within a month, the relatively slow increase in β and slow decrease in $|\alpha|$ from the mid-1970s to 2016 suggests that the coarser tail of a sand wave may take decades to transit this river segment. In fact, our measurements indicate that the bed at the LS-Lily station is continuing to coarsen, possibly still in response to the slow downstream migration of the sand wave from the last large tributary flood on Sand Creek ~50 years ago.

The sand-wave conceptual model also describes well the coupled sand-transport and grain-size processes in the more distal river segments downstream from the Little Snake River. During the late 1950s to mid-1960s period of large Sand Creek floods, the downstream migration of the resultant sand wave(s) also caused bed-sand fining in these more distal river segments, as evidenced by the increases in $|\alpha|$, rapid decreases in β, and upward shifts in the Q-C_{SAND} relations at the Green-Jensen station, ~260 km downstream from Sand Creek. Then, over the many decades following this relatively rapid bed-sand fining event, the bed sand slowly coarsened, as evidenced by the slow increases in β and downward shifts in the Q-C_{SAND} relations at the Yampa-Deerlodge and Green-Jensen stations. Thus, the signatures of the slow continued winnowing of the tail of the sand wave from the last large sand-resupplying event ~50 years ago is evident downstream in both the lower Yampa and middle Green Rivers.

It is possible that sand waves also migrated down the upper Green River before Flaming Gorge Dam, as suggested by β-detected bed-sand fining at the Green-Green River station, but data in this river segment are insufficient to conclude this with certainty. In the postdam upper Green River, it is likely that tributary-originating sand waves are present in this river segment, as evidenced by $|\alpha| \approx 1$ and short-term variation in β at the Green-Lodore station.

5.2. Implications of the Continuous Mass-Balance Sand Budgets for the Downstream Migration of Sand Waves and Geomorphic Change

The results from our continuous mass-balance sand budgets suggest that the downstream migration of sand waves in the study area is not necessarily monotonic. Under certain conditions (under different Q and/or in different river segments) these sand budgets indicate that even if the long-term trend suggests bed-sand winnowing (and associated erosion) of the tail of a sand wave, short periods of bed-sand fining (and associated accumulation) are possible. The association of sand erosion from the Deerlodge Park budget area with slight bed-sand coarsening (suggested by β) is consistent with continued winnowing of the tail of the 1950s–1960s sand wave(s) that likely originated in Sand Creek. Erosion of sand from the Deerlodge Park budget area occurred every year during 2013–2016 regardless of annual Q magnitude, thus suggesting the continued downstream progressive migration of this sand wave. The occurrence of net deposition in the Dinosaur budget area during lower-Q years, however, suggests that sand waves may bifurcate or "stall out" as a function of Q or channel geometry in certain river segments (cf. Madej & Ozaki, 1996). Although more years of data are required to know this with greater certainty, the sign of the Dinosaur annual sand budget appears to be

Table 4
Mean-Annual Loads of Total Suspended Sediment (Sand, Silt, and Clay), Suspended Silt and Clay, Suspended Sand, and Sand Bedload at Each Primary Gaging Station (in Bold) From Previous Studies and From Our 2013–2016 Measurements

Study	Mean-annual load of total suspended sediment (metric tons)	Mean-annual suspended-silt-and-clay load (metric tons)	Mean-annual suspended-sand load (metric tons)	Mean-annual sand bedload (metric tons)
Green-Lodore (postdam)				
Elliott and Anders (2005)[a]	190,000	64,000	120,000[b]	71,000[c]
Our study	200,000 ± 20,000	170,000 ± 17,000	33,000 ± 3,300	46,000 ± 23,000
Yampa-Maybell				
Andrews (1978)	380,000	---	---	110,000[cd]
Andrews (1986)	350,000	---	---	---
Grams and Schmidt (2005)	443,000	311,000[e]	132,000 ± 13,200[f]	---
Our study	210,000 ± 21,000	170,000 ± 17,000	42,000 ± 4,200	1,900 ± 1,000
LS-Lily				
Andrews (1978)	1,200,000	---	---	64,000[cd]
Andrews (1986)	1,170,000	---	---	---
Elliott and Anders (2005)[a]	370,000	200,000	73,000	61,000[c]
Grams and Schmidt (2005)	1,012,000	649,000[e]	363,000 ± 36,300[f]	291,000
Our study	560,000 ± 56,000	480,000 ± 48,000	77,000 ± 7,700	26,000 ± 13,000
Yampa-Deerlodge				
Elliott et al. (1984)[a]	1,600,000	850,000	560,000[b]	84,000[c]
Elliott and Anders (2005)[a]	g	620,000	430,000[b]	82,000[c]
Our study	830,000 ± 83,000	620,000 ± 62,000	200,000 ± 20,000[f]	68,000 ± 34,000
Green-Jensen (post-dam)				
Andrews (1986)	2,910,000	---	---	---
Elliott and Anders (2005)[a]	930,000	600,000	370,000[b]	21,000[c]
Grams and Schmidt (2005)	2,920,000	2,044,000[e]	876,000 ± 87,600[f]	---
Our study	1,200,000 ± 120,000	850,000 ± 85,000	300,000 ± 30,000	19,000 ± 10,000

[a]Mean-annual loads for the water year 2013–2016 period calculated using the sediment rating curves developed by Elliott et al. (1984) or Elliott and Anders (2005). Because a different curve was used to calculate the load in each category, the mean-annual load of total suspended sediment does not equal the sum of the mean-annual loads of silt and clay plus sand. [b]Suspended-sand load calculated by subtracting the rating-curve-predicted bedload from the rating-curve-predicted sand and gravel load. [c]Mean-annual sand bedload in these cases includes a minor amount of fine gravel. [d]Andrews (1978) calculated bedload using the Meyer-Peter and Müller (1948) bedload-transport equation. [e]Calculated by subtracting the mean-annual suspended-sand load from the mean-annual load of total suspended sediment. [f]Grams and Schmidt (2005) estimated the fraction of the total suspended sediment that was sand, with assumed 10% uncertainty. At the Yampa-Maybell and LS-Lily stations, this approach resulted in suspended-sand loads that were likely 50–70% too large. [g]Because of a typographical error in the equation in Elliott and Anders (2005), the mean-annual load for total suspended sediment at this station could not be calculated.

negatively correlated with Q. Net sand deposition occurred during years with peak $Q < 450$ m^3/s, and probable conveyance of sand occurred during years with peak Q between ~570 and 600 m^3/s. Therefore, net erosion of sand from the river segments in the Dinosaur budget area is likely only during years with peak Q greater than was observed during 2013–2016, that is, >600 m^3/s. The ~30% reduction in mean-annual peak Q caused by Flaming Gorge Dam may thus seriously limit the number of years when erosion of sand from the middle Green River is possible. This type of river-channel response is similar to that of the largely pool-drop segment of the predam Colorado River in Grand Canyon, where sand accumulated during periods of lower Q and was then eroded during the annual snowmelt flood (Topping et al., 2000).

The control of longitudinal variation in channel geometry on sediment transport will influence sediment-wave behavior, so that changes in sediment storage may be dominantly focused in shorter alluvial reaches or "sediment reservoirs" (Lisle, 2007; Lisle & Church, 2002). Thus, the changes in sand mass in our continuous sediment budgets (Table 4) are likely focused on the short alluvial reaches in our study area (Figure 1b). In the Deerlodge Park budget area, the alluvial reaches containing the largest amounts of sand are the ~4.5-km-long, ~100-m-wide lowermost Little Snake River in Lily Park and the ~8-km-long, ~250-m-wide reach of the lower Yampa River upstream from the Yampa-Deerlodge station. In the Dinosaur budget area, most sand is stored in the ~14.8-km-long (in total), ~170-m-wide (Grams & Schmidt, 2002) alluvial reaches of the middle Green River in Echo, Island, and Rainbow parks (Figure 1b), and in the short alluvial reaches of the lower Yampa River (Manners et al., 2014). If the changes in sand mass during the water year 2013-2016 period were evenly distributed in these alluvial reaches, assuming 40% bed-sand porosity (Curry et al., 2004), and given

the uncertainty bounds, these changes would correspond to between 4 and 20 cm of erosion in the alluvial reaches in the Deerlodge Park budget area and would correspond to between 9 cm of erosion and 15 cm of deposition spread evenly in the three alluvial reaches of the middle Green River. Even greater localization of these changes is the most likely scenario (e.g., Grams et al., 2013), meaning that the local amounts of erosion or deposition likely exceed these values.

5.3. Likely Sustainability of the Sand Supply in the Upper Green River and Its Effect on Sand Transport in the Middle Green River

Our results suggest that releases from Flaming Gorge Dam are exporting slightly more sand from the upper Green River in Browns Park than is being episodically resupplied by tributaries, and the introduction of annual spring floods to dam operations in 2012 (LaGory et al., 2012) has likely exacerbated this sand imbalance. Because this imbalance is slight, it remains possible, however, that little net coarsening of the bed sand has occurred at the Green-Lodore station. Although it may take a very long time because there is a large amount of predam sand in this river segment (e.g., Grams & Schmidt, 2002, 2005), the sand on the bed of the river in Browns Park will likely be slowly scoured, resulting in gradual coarsening of the bed sand. Therefore, despite the documented channel narrowing that largely occurred in two pulses in 1962 and 1983 (with little change in width since ~1994; Alexander, 2007; Grams & Schmidt, 2005; Mueller, Grams, Schmidt, Hazel, Kaplinski, et al., 2014), it is more likely that this river segment is actually in sediment deficit, as suggested by Andrews (1986) and Schmidt and Wilcock (2008). Although future bed coarsening at the Green-Lodore station would result in a reduction of the sand supplied from the upper to the middle Green River, it remains unclear what effect this possible reduction would have on sand transport in the middle Green River because this river segment currently receives roughly a factor of 3 more sand from the lower Yampa River than it does from the upper Green River. The amount of sand that accumulates in the Dinosaur budget area during lower flow years, and the associated bed sand fining, may therefore potentially offset any effects of a continued reduction in the upper Green River sand supply on sand transport in the middle Green River.

5.4. Relative Importance of Natural Coarsening Versus Dam Operations on Sand Transport

Sand transport in the middle Green River has generally decreased in response to (1) the abrupt artificial reduction in annual peak Q arising from operation of Flaming Gorge Dam, (2) the natural progressive coarsening of the bed sand caused by the continued winnowing of the tail of sand wave(s) that migrated down the Little Snake and lower Yampa rivers, and (3) the possible, though uncertain, dam-induced coarsening of the bed sand at the Green-Lodore station between 1962 and 1982. As a result of the step-change ~30% decrease in mean-annual peak Q associated with dam operations, the mean-annual suspended-sand load at the Green-Jensen station decreased by ~37% (from ~1.9 million to ~1.2 million metric tons) between the 1948–1958 predam period and the 1963–1972 early postdam period. Then, the post-1973 β-detected coarsening of the bed sand at this station resulted in a ~64% reduction in the slope of the Q-C_{SAND} relation, presumably mostly reflecting the winnowing of the tail of the sand wave(s) that likely originated in Sand Creek in the 1950s and 1960s. As a result of this increase in β, the mean-annual suspended-sand load at the Green-Jensen station decreased by ~75% (from ~1.2 million to ~300,000 metric tons) between the 1963–1972 and 2013–2016 periods. Because the more gradual post-1972 decrease in sand transport associated with bed-sand coarsening was larger than the 1959–1962 abrupt decrease in sand transport caused by the dam-induced reduction in peak Q, the natural coarsening of the bed sand has had a slightly greater influence on sand transport in the middle Green River than has operation of Flaming Gorge Dam.

5.5. Requirement of Contemporary Continuous Sediment-Transport Data

Because sediment transport in the study area has been largely in disequilibrium with the upstream sediment supply over multiyear timescales, the loads measured during our study were very different than the mean-annual loads calculated on the basis of historical daily or episodic suspended-sediment measurements (Table 4). At the gaging stations where Andrews (1978, 1986) and Grams and Schmidt (2005) calculated mean-annual suspended-sediment loads, reductions in silt-and-clay and/or sand concentration have caused factor of ~2 to 3 reductions in loads between the historical and water year 2013–2016 periods. In addition, at the gaging stations where Elliott et al. (1984) and Elliott and Anders (2005) developed sediment rating curves, changes in the sediment supply have resulted in conditions where the mean-annual silt-and-clay and

suspended-sand loads predicted by these curves can be more than a factor of 3 different than those calculated from our 2013–2016 continuous 15-min measurements (Table 4).

There is no way to know *a priori* whether sediment transport in a river has changed over time in response to changes in the upstream sediment supply. When designing monitoring programs, it should be assumed that contemporary continuous measurements of sediment transport are required to calculate accurate loads reflective of current river conditions. Only in cases where sediment transport is not affected by episodic changes in the upstream sediment supply (occurring over hours or many years) can historical sediment-transport measurements be used to calculate accurate sediment loads. Because a large investment in data collection is required to determine whether only occasional or, in fact, continuous sediment-transport measurements are required to calculate accurate sediment loads, it is perhaps more prudent to rely on contemporary continuous sediment-transport measurements until proven otherwise (e.g., Topping & Wright, 2016, p. 1–4).

6. Conclusions

Sand transport in disequilibrium with the upstream sand supply is characteristic of rivers in which large quantities of finer sand are episodically supplied from tributaries. In such cases, the sand supplied to a river during a large tributary flood moves downstream as an elongating sand wave, with substantial systematic grain-size variation in the bed, bedload, and suspension. In cases where large tributary sand-supplying floods are rare, the at-a-station coarsening associated with the downstream passage of a sand wave may persist for many decades after the last large sand-resupplying event. A novel aspect of our study has been to show how modern physically based analyses of old suspended-sand data can be used to detect the previously unrecognized passage of a sand wave through a large river network.

The changes in grain size associated with the migration of sand waves through a river network may be large enough to dominate over changes in water discharge in regulating sand transport. In particular, the natural bed-sand coarsening that has occurred in the Little Snake and lower Yampa rivers in response to the last large sand-supplying event from Sand Creek ~50 years ago has caused a slightly larger reduction in sand transport in the distal downstream middle Green River in Dinosaur National Monument than has the operation of Flaming Gorge Dam. As a result of the natural coarsening of the bed sand in the Little Snake River, lower Yampa River, and middle Green River, sand transport in this ~260-km-long combined river segment has decreased substantially since the mid-1960s and will likely continue to decrease in the future in the absence of large floods in Sand Creek. As a result of Flaming Gorge Dam modifying flows and cutting off the upstream sand supply, sand transport has also decreased in the upper Green River. Even though sand transport in this segment of the Green River has decreased largely in response to a reduction in peak discharge, it is likely that sand transport at the downstream end of this river segment exceeds the tributary resupply of sand.

Changes in sand transport have not been uniform over time and space, even though sand transport has decreased in all of these river segments, thus leading to complicated outcomes with respect to the transport of sand through different river segments. As the result of sand-wave migration, river segments can be net depositional or erosional at different times at the same water discharge. In a river segment downstream from a tributary, net deposition may occur during a large tributary flood, with net erosion of sand occurring during subsequent years (e.g., the lower Yampa River downstream from the Little Snake River). In addition, because water discharge regulates the celerity of a sand wave, certain river segments may tend toward aggradation if sand waves stall in these segments at lower discharge (e.g., the middle Green River).

In the general case, because the sources of water and sediment are in different locations in many river basins, it should not be assumed that sediment transport in a river is in equilibrium with the upstream sediment supply. Thus, sediment-transport measurement programs should rely on contemporary continuous measurements unless proven that either a sparser or historical measurement program provides estimations of sediment transport that are sufficiently accurate. This result was previously demonstrated for the Colorado River in Grand Canyon (Griffiths et al., 2012; Melis et al., 2003; Rubin et al., 2002; Topping et al., 2000; Topping & Wright, 2016) and the Rio Grande in the Big Bend region of Texas and Mexico (Dean et al., 2016). In the specific case of the rivers of Dinosaur National Monument, because these rivers have undergone major changes in sand transport driven by changes in the upstream sand supply, it is likely that future

changes in sand transport in these rivers will also be driven by changes in the upstream sand supply. Therefore, continuous measurements of sediment transport in the Little Snake, Yampa, and Green rivers will be required during any period when accurate sediment loads are required for river science or management.

Acknowledgments
The National Park Service and Bureau of Land Management funded our study. Tom Sabol, Joel Unema, and Nick Voichick of the USGS helped with data collection. Cory Williams, Rodney Richards, and Jennifer Moore of the USGS Colorado Water Science Center helped with data collection during the first year of our study. Dave Sibley, Brad Garner, Megan Hines, Eric Everman, Kathryn Schoephoester, Zackary Moore, Phethala Thongsavanh, and Tracey Reinke of the USGS all helped design the database and website for the 2012–2016 data. Jonathan Friedman, John Pitlick, John Buffington, Luca Solari, and three anonymous journal reviewers provided thoughtful comments that greatly improved the quality of this paper. Historical data used are listed in the references and supporting information; data collected during the 2012–2016 period are available at either https://www.gcmrc.gov/discharge_qw_sediment/ or https://cida.usgs.gov/gcmrc/discharge_qw_sediment/.

References

Alexander, J. (2007). The timing and magnitude of channel adjustments in the upper Green River below flaming gorge dam in Browns Park and Lodore canyon, Colorado: An analysis of the pre- and post-dam river using high-resolution dendrogeomorphology and repeat topographic surveys—Logan, Utah, Utah State University, unpublished M.S. thesis, (362 pp.).

Andrews, E.D. (1978). Present and potential sediment yields in the Yampa River basin, Colorado and Wyoming, *U.S. Geological Survey Water-Resources Investigations Report 78-105* (33 pp.). Retrieved from https://pubs.er.usgs.gov/publication/wri78105

Andrews, E. D. (1980). Effective and bankfull discharges of streams in the Yampa River basin, Colorado and Wyoming. *Journal of Hydrology*, *46*(3-4), 311–330. https://doi.org/10.1016/0022-1694(80)90084-0

Andrews, E. D. (1981). Measurement and computation of bed-material discharge in a shallow sand-bed stream, Muddy Creek, Wyoming. *Water Resources Research*, *17*(1), 131–141. https://doi.org/10.1029/WR017i001p00131

Andrews, E. D. (1986). Downstream effects of Flaming Gorge Reservoir on the Green River, Colorado and Utah. *Geological Society of America Bulletin*, *97*(8), 1,012–1,023, 10.1130/0016-7606(1986)97<1012:DEOFGR>2.0.CO;2.

Andrews, E. D. (1991). Sediment transport in the Colorado River basin, in *Commission on geosciences, environment, and resources*, *Colorado River Ecology and Dam Management* (pp. 54–74). Washington, DC: National Academy Press. Retrieved from https://www.nap.edu/download/1832

Benda, L. E. (1990). The influence of debris flows on channels and valley floors in the Oregon Coast Range, U.S.A. *Earth Surface Processes and Landforms*, *15*(5), 457–466. https://doi.org/10.1002/esp.3290150508

Bennett, J. P., & Nordin, C. F. (1977). Simulation of sediment transport and armouring. *Hydrological Sciences Bulletin*, *22*(4), 555–569. https://doi.org/10.1080/02626667709491760

Bestgen, K. R., Haines, G. B., & Hill, A. A. (2011). Synthesis of flood plain wetland information: Timing of razorback reproduction in the Green River, Utah, related to stream flow, water temperature, and flood plain wetland availability, Final report to the Upper Colorado River Endangered Fish Recovery Program, Colorado River Recovery Implementation Program Projects 22F and FR-FP Synthesis (190 pp.). Retrieved from http://www.fwspubs.org/doi/suppl/10.3996/122012-JFWM-104/suppl_file/10.3996_122012-jfwm-104.s03.pdf

Blanchard, S. F. (2007). Recent improvements to the U.S. Geological Survey streamgaging program, *U.S. Geological Survey Fact Sheet 2007–3080* (6 pp.). Retrieved from http://pubs.usgs.gov/fs/2007/3080/fs2007-3080b.pdf

Brummer, C. J., & Montgomery, D. R. (2006). Influence of coarse lag formation on the mechanics of sediment pulse dispersion in a mountain stream, Squire Creek, North Cascades, Washington, United States. *Water Resources Research*, *42*, W07412. https://doi.org/10.1029/2005WR004776

Colorado Water Conservation Board, & Colorado's Decision Support Services (2009a). Yampa River Basin information (57 pp.). Retrieved from http://cwcbweblink.state.co.us/WebLink/0/doc/146636/Electronic.aspx. (Accessed on November 23, 2016).

Colorado Water Conservation Board, & Colorado's Decision Support Services (2009b). Yampa River Basin Water Resources Planning Model User's Guide (294 pp.). Retrieved from http://cwcbweblink.state.co.us/WebLink/0/doc/146637/Electronic.aspx. (Accessed on November 23, 2016).

Cui, Y., Parker, G., Lisle, T. E., Gott, J., Hansler-Ball, M. E., Pizzuto, J. E., et al. (2003). Sediment pulses in mountain rivers: 1. Experiments. *Water Resources Research*, *39*(9), 1239. https://doi.org/10.1029/2002WR001803

Cui, Y., Parker, G., Pizzuto, J., & Lisle, T. E. (2003). Sediment pulses in mountain rivers: 2. Comparison between experiments and numerical predictions. *Water Resources Research*, *39*(9), 1240. https://doi.org/10.1029/2002WR001805

Curry, C. W., Bennett, R. H., Hulbert, M. H., Curry, K. J., & Faas, R. W. (2004). Comparative study of sand porosity and a technique for determining porosity of undisturbed marine sediment. *Marine Georesources and Geotechnology*, *22*(4), 231–252. https://doi.org/10.1080/10641190490900844

Davis, J. C. (1986). *Statistics and data analysis in geology* (2nd ed. 646 pp.). New York: John Wiley.

Dean, D. J., Topping, D. J., Schmidt, J. C., Griffiths, R. E., & Sabol, T. A. (2016). Sediment supply versus local hydraulic controls on sediment transport and storage in a river with large sediment loads. *Journal of Geophysical Research: Earth Surface*, *121*, 82–110. https://doi.org/10.1002/2015JF003436

Dietrich, W. E., & Dunne, T. (1978). Sediment budget for a small catchment in mountainous terrain. *Zeitschrift für Geomorphologie*, *29*, 191–206.

Dinehart, R. L. (1998). Sediment transport at gaging stations near Mount St. Helens, Washington, 1980–90, data collection and analysis, *U.S. Geological Survey Professional Paper 1573*, (111 pp.). Retrieved from https://pubs.usgs.gov/pp/1573/

Dolan, L. S., & Wesche, T. A. (1987). Summary of Muddy Creek surface water and sediment transport data 1984–1986, *Technical Report WWRC-87-28*, Wyoming Research Center, University of Wyoming, Laramie, Wyoming (57 pp.). Retrieved from http://library.wrds.uwyo.edu/wrp/87-28/87-28.pdf

Edwards, T.K., & G. D. Glysson (1999). Field methods for measurement of fluvial sediment, *Techniques of Water-Resources Investigations of the U.S. Geological Survey* (book 3, chapter C2, 89 pp.). Retrieved from https://pubs.usgs.gov/twri/twri3-c2/

Einstein, H. A. (1950). The bed-load function for sediment transportation in open channel flows, U.S. Department of Agriculture, soil conservation service, Technical Bulletin No. 1026 (71 pp.). Retrieved from https://naldc.nal.usda.gov/download/CAT86201017/PDF

Einstein, H. A., & Chien, N. (1953). Transport of sediment mixtures with large ranges of grain size, *Missouri River District Sediment Series* (Vol. *2*, 72 pp.). Berkeley: University of California.

Elliott, J. G., & Anders, S. P. (2005). Summary of sediment data from the Yampa River and upper Green River Basins, Colorado and Utah, 1993–2002, *U.S. Geological Survey Scientific Investigations Report 2004-5242* (35 pp.). Retrieved from https://pubs.er.usgs.gov/publication/sir20045242

Elliott, J. G., Kircher, J. E., & Von Guerard, P. (1984). Sediment transport in the lower Yampa River, northwestern Colorado, *U.S. Geological Survey Water-Resources Investigations Report 84-414* (44 pp.). Retrieved from https://pubs.er.usgs.gov/publication/wri844141

Exner, F. M. (1920). Zur physik der dünen. *Akad. Wiss. Wien Math.-Naturwiss. Kl. Sitzungsber. Abt. IIa*, *134*(2a), 165–204.

Exner, F. M. (1925). Uber die wechselwirkung zwischen wasser und geschiebe in flüssen. *Akad. Wiss. Wien Math.-Naturwiss. Kl. Sitzungsber. Abt. IIa*, *134*, 165–203.

Federal Interagency Sedimentation Project (1952). Report 6: The design of improved types of suspended sediment samplers, *A study of methods used in measurement and analysis of sediment loads in streams* (103 pp.). Minneapolis, Minnesota: St. Anthony Falls Hydraulic Laboratory. Retrieved from http://water.usgs.gov/fisp/docs/Report_6.pdf

Ferguson, R. I., Church, M., Rennie, C. D., & Venditti, J. G. (2015). Reconstructing a sediment pulse: Modeling the effect of placer mining on Fraser River, Canada. *Journal of Geophysical Research: Earth Surface*, *120*, 1436–1454. https://doi.org/10.1002/2015JF003491

Fernandez Luque, R., & van Beek, R. (1976). Erosion and transport of bed-load sediment. *Journal of Hydraulic Research*, *14*(2), 127–144. https://doi.org/10.1080/00221687609499677

Fischer, H. B. (1973). Longitudinal dispersion and turbulent mixing in open channel flow. *Annual Review of Fluid Mechanics*, *5*, 289–302. https://doi.org/10.1146/annurev.fl.05.010173.000423

Garcia, M., & Parker, G. (1991). Entrainment of bed sediment into suspension. *Journal of Hydraulic Engineering*, *117*(4), 414–435. https://doi.org/10.1061/(ASCE)0733-9429(1991)117:4(414)

Grams, P. E., & Schmidt, J. C. (1999). Geomorphology of the Green River in the eastern Uinta Mountains, Dinosaur National Monument, Colorado and Utah. In A. J. Miller, & A. Gupta (Eds.), *Varieties of Fluvial Form* (pp. 81–111). Chichester, UK: John Wiley.

Grams, P. E., & Schmidt, J. C. (2002). Streamflow regulation and multi-level flood plain formation: Channel narrowing on the aggrading Green River in the eastern Uinta Mountains, Colorado and Utah. *Geomorphology*, *22*(3–4), 337–360. https://doi.org/10.1016/S0169-555X(01)00182-9

Grams, P. E., & Schmidt, J. C. (2005). Equilibrium or indeterminate? Where sediment budgets fail: Sediment mass balance and adjustment of channel form, Green River downstream from Flaming Gorge Dam, Utah and Colorado. *Geomorphology*, *71*(1–2), 156–181. https://doi.org/10.1016/j.geomorph.2004.10.012

Grams, P. E., Topping, D. J., Schmidt, J. C., Hazel, J. E. Jr., & Kaplinski, M. (2013). Linking morphodynamic response with sediment mass balance on the Colorado River in Marble Canyon: Issues of scale, geomorphic setting, and sampling design. *Journal of Geophysical Research: Earth Surface*, *118*, 361–381. https://doi.org/10.1002/jgrf.20050

Gran, K. B., Montgomery, D. R., & Halbur, J. C. (2011). Long-term elevated post-eruption sedimentation at Mount Pinatubo, Philippines. *Geology*, *39*(4), 367–370. https://doi.org/10.1130/G31682.1

Gray, J. R., & Gartner, J. W. (2009). Technological advances in suspended-sediment surrogate monitoring. *Water Resources Research*, *45*, W00D29. https://doi.org/10.1029/2008WR007063

Gray, J. R., & Simoes, F. J. M. (2008). Estimating sediment discharge, Appendix D. In M. H. Garcia (Ed.), *Sedimentation Engineering – Processes, Measurements, Modeling, and Practice, American Society of Civil Engineers Manuals and Reports on Engineering Practice* (Vol. 110, pp. 1067–1088). Reston, VA: American Society of Civil Engineers.

Griffiths, R. E., & Topping, D. J. (2017). Importance of measuring discharge and sediment transport in lesser tributaries when closing sediment budgets. *Geomorphology*, *296*, 59–73. https://doi.org/10.1016/j.geomorph.2017.08.037

Griffiths, R. E., Topping, D. J., Andrews, T., Bennett, G. E., Sabol, T. A., & Melis, T. S. (2012). Design and maintenance of a network for collecting high-resolution suspended-sediment data at remote locations on rivers, with examples from the Colorado River, *U.S. Geological Survey Techniques and Methods 8-C2* (44 pp.). Retrieved from http://pubs.usgs.gov/tm/tm8c2/

Guy, H. P. (1970). Fluvial sediment concepts, *U.S. Geological Survey Techniques of Water-Resources Investigations*, (book 3, chapter C1, 55 pp.). Retrieved from http://pubs.usgs.gov/twri/twri3-c1/

Howard, A., & Dolan, R. (1981). Geomorphology of the Colorado River in the Grand Canyon. *Journal of Geology*, *89*(3), 269–298. https://doi.org/10.1086/628592

Iorns, W. V., Hembree, C. H., Phoenix, D. A., & Oakland, G. L. (1964). Water resources of the Upper Colorado River Basin—Basic data, *U.S. Geological Survey Professional Paper 442*, 1,036 pp. and 12 plates. Retrieved from https://pubs.er.usgs.gov/publication/pp442

James, L. A. (2006). Bed waves at the basin scale: Implications for river management and restoration. *Earth Surface Processes and Landforms*, *31*, 1692–1706. https://doi.org/10.1002/esp.1432

James, L. A. (2010). Secular sediment waves, channel bed waves, and legacy sediment. *Geography Compass*, *4/6*, 576–598. https://doi.org/10.1111/j.1749-8198.2010.00324.x

Kiang, J. E., Mason, R. R., & Cohn, T. A. (2016). A survey of the uncertainty in stage-discharge rating curves and streamflow records in the United States. In G. Constantinescu, M. Garcia, & D. Hanes (Eds.), *River Flow 2016, CD-ROM Proceedings of the International Conference on Fluvial Hydraulics* (pp. 724–728). St. Louis, Missouri. July 11–14, 2016, ISBN 978–1–138-2913-2 for set of Book and CD-ROM, ISBN 978–1–315-64447-9 for eBook PDF, on CD-ROM, New York: CRC Press, Taylor & Francis Group.

LaGory, K., Chart, T., Bestgen, K., Wilhite, J., Capron, S., Speas, D., et al. (2012). Study plan to examine the effect of using larval razorback sucker occurrence in the Green River as a trigger for Flaming Gorge Dam peak releases, Final report to the Upper Colorado River Endangered Fish Recovery Program (24 pp.). Retrieved from https://www.fws.gov/Region6Test/documents-publications/technical-reports/isf/larvaltrig-gerstudyplan.pdf

Linenburger, T. R. (1997). Seedskadee Project, Bureau of Reclamation History Program, Denver, Colorado, Research on Historic Reclamation Projects (38 pp.). Retrieved from https://www.usbr.gov/projects/pdf.php?id=191

Linenburger, T. R. (1998). Flaming Gorge Unit, Colorado River Storage Project, Bureau of Reclamation History Program, Denver, Colorado, Research on Historic Reclamation Projects (34 pp.). Retrieved from https://www.usbr.gov/projects/pdf.php?id=85

Lisle, T. E. (2007). The evolution of sediment waves influenced by varying transport capacity in heterogeneous rivers, in H. Habersack, H. Piegay, M. Rinaldi, (Eds.), Gravel-Bed Rivers VI: From Process Understanding to River Restoration. *Developments in Earth Surface Processes*, *11*, 443–469. https://doi.org/10.1016/S0928-2025(07)11136-6

Lisle, T. E., & Church, M. (2002). Sediment transport-storage relations for degrading, gravel bed channels. *Water Resources Research*, *38*(11), 1219. https://doi.org/10.1029/2001WR001086

Madej, M. A., & Ozaki, V. (1996). Channel response to sediment wave propagation and movement, Redwood Creek, California, USA. *Earth Surface Processes and Landforms*, *21*(10), 911–927. https://doi.org/10.1002/(SICI)1096-9837(199610)21:10%3C911::AID-ESP621%3E3.0.CO;2-1

Major, J. J. (2004). Posteruption suspended sediment transport at Mount St. Helens: Decadal-scale relationships with landscape adjustments and river discharges. *Journal of Geophysical Research*, *109*, F01002. https://doi.org/10.1029/2002JF000010

Mann, H. B., & Whitney, D. R. (1947). On a test of whether one of two random variables is stochastically larger than the other. *Annals of Mathematical Statistics*, *18*(1), 50–60. https://doi.org/10.1214/aoms/1177730491

Manners, R. B., Schmidt, J. C., & Scott, M. L. (2014). Mechanisms of vegetation-induced channel narrowing of an unregulated canyon river: Results from a natural field-scale experiment. *Geomorphology*, *211*, 100–115. https://doi.org/10.1016/j.geomorph.2013.12.033

Martin, J. A., Grams, P. E., Kammerer, M. T., & Schmidt, J. C. (1998). Sediment transport and channel response of the Green River in the Canyon of Lodore between 1995–1997, including measurements during high flows, Dinosaur National Monument, Colorado, Draft Final Report to National Park Service and Bureau of Reclamation, Utah State University Cooperative Agreements 1268–1-9006 (National Park Service) and 1425–97-FC-40_21650 (Bureau of Reclamation) (190 pp.).

McLean, S. R. (1992). On the calculation of suspended load for noncohesive sediments. *Journal of Geophysical Research*, *97*, 5,759–5,770. https://doi.org/10.1029/JC082i012p01735

Melis, T. S., Topping, D. J., & Rubin, D. M. (2003). Testing laser-based sensors for continuous in situ monitoring of suspended sediment in the Colorado River, Arizona, In Bogen, J., Fergus, T., & Walling, D. E. (Eds.), *Erosion and sediment transport measurement in rivers: Technological and methodological advances*, *IAHS Publication* (283, 21–27). Wallingford, Oxfordshire, United Kingdom: IAHS Press. Retrieved from http://hydrologie.org/redbooks/a283/iahs_283_021.pdf

Meyer-Peter, E., & Müller, R. (1948). Formulas for bed-load transport, Proceedings of the 2nd Meeting of the IAHR, Stockholm, 39-64.

Mueller, E. R., Grams, P. E., Schmidt, J. C., Hazel, J. E. Jr., Alexander, J. S., & Kaplinski, M. (2014). The influence of controlled floods on fine sediment storage in debris fan-affected canyons of the Colorado River basin. *Geomorphology*, *226*, 65–75. https://doi.org/10.1016/j.geomorph.2014.07.029

Mueller, E. R., Grams, P. E., Schmidt, J. C., Hazel, J. E. Jr., Kaplinski, M., Alexander, J. S., & Kohl, K. (2014). Monitoring and research to describe geomorphic effects of the 2011 controlled flood on the Green River in the Canyon of Lodore, Dinosaur National Monument, Colorado and Utah, *U.S. Geological Survey Science Investigations Report 2014–5022* (66 pp.). https://doi.org/10.3133/sir20145022

Oberg, K., & Mueller, D. S. (2007). Validation of streamflow measurements made with acoustic Doppler current profilers. *Journal of Hydraulic Engineering*, *133*(12), 1421–1432. https://doi.org/10.1061/(ASCE)0733-9429(2007)133:12(1421)

O'Brien, J. S. (1984). Hydraulic and sediment transport investigation, Yampa River, Dinosaur National Monument, Fort Collins, Colorado State University, National Park Service Water Resources Field Support Laboratory, Final Report WRFSL Report No. 83-8, (86 pp.).

Osterkamp, W. R., & Parker, R. S. (1991). Sediment monitoring in the United States, *Proceedings of the 5th Federal Interagency Sedimentation Conference*, Las Vegas, Nevada, 1991, (Vol. 1, pp. 1–15 to 1–23).

Parker, G. (1978). Self-formed straight rivers with equilibrium banks and mobile bed. Part 1: The sand-silt river. *Journal of Fluid Mechanics*, *89*(01), 109–125. https://doi.org/10.1017/S0022112078002499

Parker, G. (2008). Transport of gravel and sediment mixtures, Chapter 3. In M. H. Garcia (Ed.), *Sedimentation engineering—Processes, measurements, modeling, and practice, American Society of Civil Engineers Manuals and Reports on Engineering Practice* (Vol. 110, pp. 165–251). Reston, VA: American Society of Civil Engineers.

Parker, M., Wood, F. J. Jr., Smith, B. H., & Elder, R. G. (1985). Erosional downcutting in lower order riparian ecosystems: Have historical changes been caused by removal of beaver? In R. R. Johnson, et al., (Eds.), *Riparian ecosystems and their management: Reconciling conflicting uses, First North American Riparian Conference, University of Arizona, Tucson*, *USDA Forest Service General Technical Report RM-120* (35–38). Fort Collins, CO: Rocky Mountain Forest and Range Experiment Station. Retrieved from http://www.fs.fed.us/rm/pubs_rm/rm_gtr120/rm_gtr120_035_038.pdf

Porterfield, G. (1972). Computation of fluvial sediment discharge, U.S. Geological Survey Techniques of Water-Resources Investigations, book 3, chapter C3, 66 pp.

Rantz, S. E., et al. (1982a). Measurement and computation of streamflow: Volume 1. Measurement of stage and discharge, *U.S. Geological Survey Water-Supply Paper 2175*, 1–284. Retrieved from https://pubs.usgs.gov/wsp/wsp2175/pdf/WSP2175_vol1a.pdf

Rantz, S. E., et al. (1982b). Measurement and computation of streamflow: Volume 2. Computation of discharge, *U.S. Geological Survey Water-Supply Paper 2175*, 285–631. Retrieved from https://pubs.usgs.gov/wsp/wsp2175/pdf/WSP2175_vol2a.pdf

Resource Consultants (1991). Sediment transport studies of the Little Snake, Yampa, and Green River systems, Final report to Colorado River Water Conservation District, Glenwood Springs, CO, and Wyoming Water Development Commission, Cheyenne, WY, Reference 90–478, 187 pp. including 7 appendices, accessed on August 29, 2016, http://library.wrds.uwyo.edu/wwdcrept/Little_Snake/Little_Snake_R-Sediment_Transport_Studies_Yampa_and_Green_River_Systems-Final_Report-1991.pdf

Rouse, H. (1937). Modern conceptions of mechanics of fluid turbulence. *Transactions of the American Society of Civil Engineers*, *102*, 463–505.

Rubin, D. M., Nelson, J. M., & Topping, D. J. (1998). Relation of inversely graded deposits to suspended-sediment grain-size evolution during the 1996 Flood Experiment in Grand Canyon. *Geology*, *26*, 99–102. https://doi.org/10.1130/0091-7613(1998)026<0099:ROIGDT>2.3.CO;2

Rubin, D. M., & Topping, D. J. (2001). Quantifying the relative importance of flow regulation and grain-size regulation of suspended-sediment transport (α), and tracking changes in bed-sediment grain size (β). *Water Resources Research*, *37*, 133–146. https://doi.org/10.1029/2000WR900250

Rubin, D. M., & Topping, D. J. (2008). Correction to "Quantifying the relative importance of flow regulation and grain-size regulation of suspended-sediment transport α, and tracking changes in bed-sediment grain size β". *Water Resources Research*, *44*, W09701. https://doi.org/10.1029/2008WR006819

Rubin, D. M., Topping, D. J., Schmidt, J. C., Hazel, J., Kaplinski, M., & Melis, T. S. (2002). Recent sediment studies refute Glen Canyon Dam hypothesis. *Eos, Transactions of the American Geophysical Union*, *83*(25), 273–278. https://doi.org/10.1029/2002EO000191

Sabol, T. A., & Topping, D. J. (2013). Evaluation of intake efficiencies and associated sediment-concentration errors in US D-77 bag-type and US D-96-type depth-integrating suspended-sediment samplers, *U.S. Geological Survey Scientific Investigations Report 2012–5208* (88 pp.). https://doi.org/10.3133/sir20125208.

Sauer, V. B., & Meyer, R. W. (1992). Determination of error in individual discharge measurements, *U.S. Geological Survey Open-File Report 92–144* (21 pp.). Retrieved from http://pubs.usgs.gov/of/1992/ofr92-144/

Schmeeckle, M. W. (2014). Numerical simulation of turbulence and sediment transport of medium sand. *Journal of Geophysical Research - Earth Surface*, *119*, 1240–1262. https://doi.org/10.1002/2013JF002911

Schmeeckle, M. W., & Nelson, J. M. (2003). Direct numerical simulation of bedload transport using a local, dynamic boundary condition. *Sedimentology*, *20*(2), 279–301. https://doi.org/10.1046/j.1365-3091.2003.00555.x

Schmidt, J. C., & Wilcock, P. R. (2008). Metrics for assessing the downstream effects of dams. *Water Resources Research*, *44*, W04404. https://doi.org/10.1029/2006WR005092

Sibley, D., D. J. Topping, M. Hines, & B. Garner (2015). User-interactive sediment budgets in a browser: A web application for river science and management, *Proceedings of the 3rd Joint Federal Interagency Conference on Sedimentation and Hydrologic Modeling*, April 19-23, 2015, Peppermill Hotel, Reno, Nevada (pp. 595–605). Retrieved from http://acwi.gov/sos/pubs/3rdJFIC/Proceedings.pdf

Simons, D. B., E. V. Richardson, & C. F. Nordin (1965). Bedload equation for ripples and dunes, *U.S. Geological Survey Professional Paper 462-H*, (9 pp.). Retrieved from https://pubs.er.usgs.gov/publication/pp462H

Sklar, L. S., Fadde, J., Venditti, J. G., Nelson, P., Wydzga, M. A., Cui, Y., & Dietrich, W. E. (2009). Translation and dispersion of sediment pulses in flume experiments simulating gravel augmentation below dams. *Water Resources Research*, *45*, W08439. https://doi.org/10.1029/2008WR007346

Smith, J. D., & McLean, S. R. (1977). Spatially averaged flow over a wavy surface. *Journal of Geophysical Research*, *82*, 1735–1746. https://doi.org/10.1029/JC082i012p01735

Topping, D. J., Rubin, D. M., Grams, P. E., Griffiths, R. E., Sabol, T. A., Voichick, N., et al. (2010). Sediment transport during three controlled-flood experiments on the Colorado River downstream from Glen Canyon Dam, with implications for eddy-sandbar deposition in Grand Canyon National Park, *U.S. Geological Survey Open-File Report 2010–1128* (111 pp.). Retrieved from http://pubs.usgs.gov/of/2010/1128/

Topping, D. J., Rubin, D. M., & Melis, T. S. (2007). Coupled changes in sand grain size and sand transport driven by changes in the upstream supply of sand in the Colorado River: Relative importance of changes in bed-sand grain size and bed-sand area. *Sedimentary Geology*, *202*(3), 538–561. https://doi.org/10.1016/j.sedgeo.2007.03.016

Topping, D. J., Rubin, D. M., Nelson, J. M., Kinzel, P. J. III., & Corson, I. C. (2000). Colorado River sediment transport: 2. Systematic bed-elevation and grain-size effects of sand supply limitation. *Water Resources Research*, *36*, 543–570. https://doi.org/10.1029/1999WR900286

Topping, D. J., Rubin, D. M., & Vierra, L. E. Jr. (2000). Colorado River sediment transport: 1. Natural sediment supply limitation and the influence of Glen canyon dam. *Water Resources Research*, *36*, 515–542. https://doi.org/10.1029/1999WR900285

Topping, D. J., D. M. Rubin, S. A. Wright, & T. S. Melis (2011). Field evaluation of the error arising from inadequate time averaging in the standard use of depth-integrating suspended-sediment samplers, *U.S. Geological Survey Professional Paper 1774* (95 pp.). Retrieved from http://pubs.usgs.gov/pp/1774/

Topping, D. J., & Wright, S. A. (2016). Long-term continuous acoustical suspended-sediment measurements in rivers—Theory, application, bias, and error, *U.S. Geological Survey Professional Paper 1823* (98 pp.). https://doi.org/10.3133/pp1823

Topping, D. J., Wright, S. A., Griffiths, R. E., & Dean, D. J. (2016). Long-term continuous acoustical suspended-sediment measurements in rivers—Theory, evaluation, and results from 14 stations on five rivers. In G. Constantinescu, M. Garcia, & D. Hanes (Eds.), *River Flow 2016, CD-ROM Proceedings of the International Conference on Fluvial Hydraulics* (pp. 1510–1518). St. Louis, Missouri. July 11–14, 2016, ISBN 978–1–138-2913-2 for set of Book and CD-ROM, ISBN 978–1–315-64447-9 for eBook PDF, New York: CRC Press, Taylor & Francis Group.

Turnipseed, D. P., & Sauer, V. B. (2010). Discharge measurements at gaging stations, *U.S. Geological Survey Techniques and Methods 3-A8*, (87 pp.). Retrieved from http://pubs.usgs.gov/tm/tm3-a8/

U.S. Bureau of Reclamation (2006). Record of decision, Operation of Flaming Gorge Dam, Final Environmental Impact Statement. Retrieved from https://www.usbr.gov/uc/envdocs/rod/fgFEIS/final-ROD-15feb06.pdf

U.S. Bureau of Reclamation (2016). Colorado River Basin natural flow and salt data. Retrieved from https://www.usbr.gov/lc/region/g4000/NaturalFlow/current.html, (accessed on January 30, 2017).

U.S. Department of Agriculture (1981). Cheyenne State II Water Diversion Proposal, Final Environmental Impact Statement and Record of Decision, 464 pp. Retrieved from https://books.google.com/books?id=iTw3AQAAMAAJ&pg=PP7&dq=Cheyenne+State+II+Water+Diversion+Proposal,+Final+Environmental+Impact+Statement+and+Record+of+Decision&hl=en&sa=X&ved=0ahUKEwjZ6qH50IHcAhXCxVkKHS6WDfMQ6AEIJzAA#v=onepage&q=Cheyenne%20State%20II%20Water%20Diversion%20Proposal%2C%20Final%20Environmental%20Impact%20Statement%20and%20Record%20of%20Decision&f=false

U.S. Department of the Interior (2005). Operation of Flaming Gorge Dam, Final Environmental Impact Statement. Retrieved from https://www.usbr.gov/uc/envdocs/eis/fgFEIS/index.html

U.S. Environmental Protection Agency (2014). Constructed wetlands control sedimentation in Wyoming's Muddy Creek, *Section 319*, *Nonpoint source program success story*, EPA 841-F-14-001SS. Retrieved from https://www.epa.gov/sites/production/files/2015-10/documents/wy_lowermuddy.pdf

U.S. Geological Survey (2017a). Peak streamflow for the nation, USGS, 09258900, Muddy Creek above Baggs, WY. Retrieved from https://nwis.waterdata.usgs.gov/nwis/peak/?site_no=09258900&agency_cd=USGS&amp, (accessed on January 30, 2017).

U.S. Geological Survey (2017b). Peak streamflow for the nation, USGS, 09259000, Muddy Creek near Baggs, WY. Retrieved from https://nwis.waterdata.usgs.gov/nwis/peak/?site_no=09259000&agency_cd=USGS&amp, (accessed on January 30, 2017).

U.S. Geological Survey (2017c). Peak streamflow for the nation, USGS, 09258980, Muddy Creek below Young Draw, near Baggs, WY. Retrieved from https://nwis.waterdata.usgs.gov/nwis/peak/?site_no=09258980&agency_cd=USGS&amp, (accessed on January 30, 2017).

U.S. Geological Survey (2017d). Water quality samples for the nation, USGS, 412325107244101, Muddy C ab Canary Grove Draw nr Baggs, WY. Retrieved from https://nwis.waterdata.usgs.gov/nwis/qwdata/?site_no=412325107244101&agency_cd=USGS&amp, (accessed on January 30, 2017).

U.S. Geological Survey (2017e). Water quality samples for the nation, USGS, 412614107452101, Muddy C nr Dad WY. Retrieved from https://nwis.waterdata.usgs.gov/nwis/qwdata/?site_no=412614107452101&agency_cd=USGS&amp, (accessed on January 30, 2017).

U.S. Geological Survey (2017f). Water quality samples for the nation, USGS, 09258900 Muddy Creek above Baggs, WY. Retrieved from https://nwis. waterdata.usgs.gov/nwis/qwdata/?site_no=09258900&agency_cd=USGS&amp, (accessed on January 30, 2017).

U.S. Geological Survey (2017g). Water quality samples for the nation, USGS, 09259000, Muddy Creek near Baggs, WY. Retrieved from https://nwis.waterdata.usgs.gov/nwis/qwdata/?site_no=09259000&agency_cd=USGS&amp, (accessed on January 30, 2017).

U.S. Geological Survey (2017h). Water quality samples for the nation, USGS, 411134108102002, Sand C ab Skull C nr Prehistoric Rim. Retrieved from https://nwis.waterdata.usgs.gov/nwis/qwdata/?site_no=411134108102002&agency_cd=USGS&amp, (accessed on January 30, 2017).

U.S. Geological Survey (2017i). Water quality samples for the nation, USGS, 410229107521601, Sand Creek, nr Baggs, WY. Retrieved from https://nwis.waterdata.usgs.gov/nwis/qwdata/?site_no=410229107521601&agency_cd=USGS&amp, (accessed on January 30, 2017).

Van Rijn, L. C. (1984a). Sediment transport. Part II: Suspended load transport. *Journal of Hydraulic Engineering*, *110*(11), 1613–1641. https://doi.org/10.1061/(ASCE)0733-9429(1984)110:11(1613)

Van Rijn, L. C. (1984b). Sediment transport. Part I: Bed load transport. *Journal of Hydraulic Engineering*, *110*(10), 1431–1456. https://doi.org/10.1061/(ASCE)0733-9429(1984)110:10(1431)

Venditti, J. G., Dietrich, W. E., Nelson, P. A., Wydzga, M. A., Fadde, J., & Sklar, L. (2010). Effect of sediment pulse grain size on sediment transport rates and bed mobility in gravel bed rivers. *Journal of Geophysical Research*, *115*, F03039. https://doi.org/10.1029/2009JF001418

Vinson, M. R. (2001). Long-term dynamics of an invertebrate assemblage downstream from a large dam. *Ecological Applications*, *11*(3), 711–730. https://doi.org/10.1890/1051-0761(2001)011[0711:LTDOAI]2.0.CO;2

White, M. A., Schmidt, J. C., & Topping, D. J. (2005). Application of wavelet analysis for monitoring the hydrologic effects of dam operation: Glen Canyon Dam and the Colorado River at Lees Ferry, Arizona. *River Research and Applications*, *21*, 551–565. https://doi.org/10.1002/rra.827

Wiberg, P. L., & Smith, J. D. (1989). Model for calculating bed load transport of sediment. *Journal of Hydraulic Engineering*, *115*(1), 101–123. https://doi.org/10.1061/(ASCE)0733-9429(1989)115:1(101)

Wilcock, P. R., & McArdell, B. W. (1993). Surface-based fractional transport rates: Mobilization thresholds and partial transport of a sand-gravel sediment. *Water Resources Research*, *29*, 1297–1312. https://doi.org/10.1029/92WR02748

Wilcock, P. R., & Southard, J. B. (1989). Bed load transport of mixed size sediment: Fractional transport rates, bed forms, and the development of a coarse bed surface layer. *Water Resources Research*, *25*, 1629–1641. https://doi.org/10.1029/WR025i007p01629

Wohl, E. E., & Cenderelli, D. A. (2000). Sediment deposition and transport patterns following a reservoir sediment release. *Water Resources Research*, *36*, 319–333. https://doi.org/10.1029/1999WR900272

Wright, S. A., Topping, D. J., Rubin, D. M., & Melis, T. S. (2010). An approach for modeling sediment budgets in supply-limited rivers. *Water Resources Research*, *46*, W10538. https://doi.org/10.1029/2009WR008600

Wyoming Water Planning Program, State Engineer's Office (1978). Summary and analysis of the City of Cheyenne's proposed Stage II water system expansion, (41 pp.). Retrieved from http://library.wrds.uwyo.edu/wwpp/UN-Summary_and_Analysis_of_the_City_of_Cheyennes_Porposed_Stage_II_Water_System_Expansion.html

Yalin, M. S. (1963). An expression for bed load transportation. *Journal of Hydraulics Division, ASCE*, *89*(3), 221–250.